

RD-A154 889

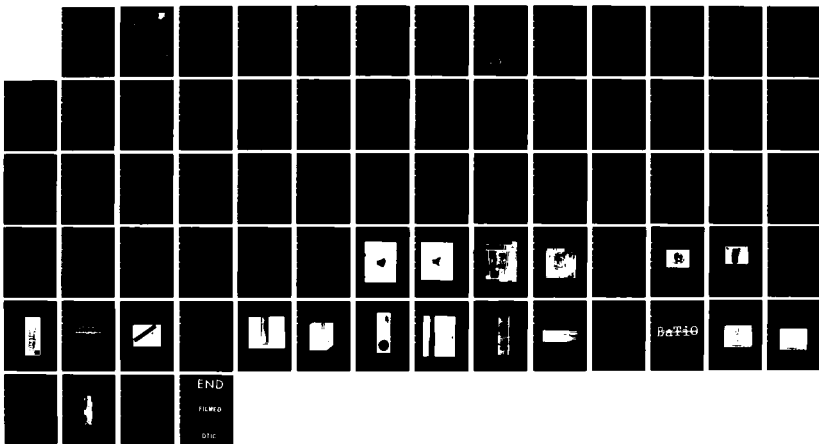
DEVELOPMENT OF GROWTH TECHNIQUES FOR ELECTROMAGNETIC
CRYSTALS(U) STANFORD UNIV CA CENTER FOR MATERIALS
RESEARCH R S FEIGELSON ET AL. FEB 85 RADC-TR-85-33
F19628-81-K-0047 F/G 20/2

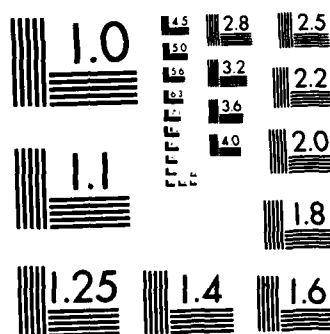
1/1

UNCLASSIFIED

F/G 20/2

NL





MICROCOPY RESOLUTION TEST CHART
NATIONAL BUREAU OF STANDARDS-1963-A

2

RADC-TR-85-33
Final Technical Report
February 1985



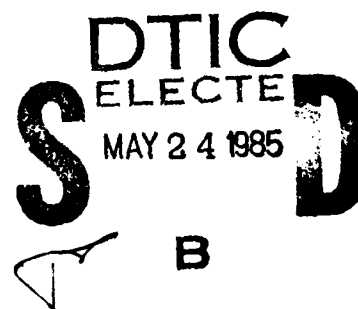
DEVELOPMENT OF GROWTH TECHNIQUES FOR ELECTROMAGNETIC CRYSTALS

Stanford University

Professor R. S. Feigelson
Dr. Roger K. Route
Mr. Wayne L. Kway

APPROVED FOR PUBLIC RELEASE; DISTRIBUTION UNLIMITED

DTIC FILE COPY



ROME AIR DEVELOPMENT CENTER
Air Force Systems Command
Griffiss Air Force Base, NY 13441-5700

85 04 30 047

This report has been reviewed by the RADC Public Affairs Office (PA) and is releasable to the National Technical Information Service (NTIS). At NTIS it will be releasable to the general public, including foreign nations.

RADC-TR-85-33 has been reviewed and is approved for publication.

APPROVED:



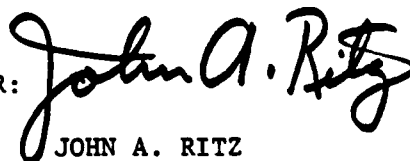
JOHN J. LARKIN
Project Engineer

APPROVED:



HAROLD ROTH, Director
Solid State Sciences Division

FOR THE COMMANDER:



JOHN A. RITZ
Acting Chief, Plans Office

If your address has changed or if you wish to be removed from the RADC mailing list, or if the addressee is no longer employed by your organization, please notify RADC () Hanscom AFB MA 01731. This will assist us in maintaining a current mailing list.

Do not return copies of this report unless contractual obligations or notices on a specific document requires that it be returned.

UNCLASSIFIED

SECURITY CLASSIFICATION OF THIS PAGE

AD-A154089

REPORT DOCUMENTATION PAGE

1a. REPORT SECURITY CLASSIFICATION UNCLASSIFIED			1b. RESTRICTIVE MARKINGS N/A		
2a. SECURITY CLASSIFICATION AUTHORITY N/A			3. DISTRIBUTION/AVAILABILITY OF REPORT Approved for public release; distribution unlimited		
2b. DECLASSIFICATION/DOWNGRADING SCHEDULE N/A					
4. PERFORMING ORGANIZATION REPORT NUMBER(S) N/A			5. MONITORING ORGANIZATION REPORT NUMBER(S) RADC-TR-85-33		
6a. NAME OF PERFORMING ORGANIZATION Stanford University		6b. OFFICE SYMBOL (If applicable)		7a. NAME OF MONITORING ORGANIZATION Rome Air Development Center (ESME)	
6c. ADDRESS (City, State and ZIP Code) McCullough Building Center for Materials Research Stanford CA 94305			7b. ADDRESS (City, State and ZIP Code) Hanscom AFB MA 01731		
8a. NAME OF FUNDING/SPONSORING ORGANIZATION Rome Air Development Center		8b. OFFICE SYMBOL (If applicable) ESME		9. PROCUREMENT INSTRUMENT IDENTIFICATION NUMBER F19628-81-K-0047	
8c. ADDRESS (City, State and ZIP Code) Hanscom AFB MA 01731-5700			10. SOURCE OF FUNDING NOS.		
			PROGRAM ELEMENT NO. 62702F	PROJECT NO. 4600	TASK NO. 17
			WORK UNIT NO. 48		
11. TITLE (Include Security Classification) DEVELOPMENT OF GROWTH TECHNIQUES FOR ELECTROMAGNETIC CRYSTALS					
12. PERSONAL AUTHOR(S) Professor R.S. Feigelson, Dr. Roger K. Route, Mr. Wayne L. Kway					
13a. TYPE OF REPORT Final		13b. TIME COVERED FROM Sep 81 TO Sep 84		14. DATE OF REPORT (Yr., Mo., Day) February 1985	
15. PAGE COUNT					
16. SUPPLEMENTARY NOTATION N/A					
17. COSATI CODES			18. SUBJECT TERMS (Continue on reverse if necessary and identify by block number)		
FIELD	GROUP	SUB. GR.	crystal growth Laser Heating Fibers Pedestal Heating		
20	02				
20	04				
19. ABSTRACT (Continue on reverse if necessary and identify by block number) Techniques were developed for growth of single crystal fibers using a laser pedestal heating system. Oriented growth of refractory fibers was demonstrated for oxides, semi-conductors, and some metals. Since no crucible is used to contain the feed material, and only the tip of the pedestal material is melted, purity control is excellent. Controlled atmosphere growth and the design of retroreflectors to optimize laser power were investigated. This type of laser heated pedestal system appears to be appropriate for almost any material which does not have an excessively high vapor pressure at the melting point. Difficulties in growing refractory metals should be surmounted by using higher laser powers. None included					
20. DISTRIBUTION/AVAILABILITY OF ABSTRACT UNCLASSIFIED/UNLIMITED <input checked="" type="checkbox"/> SAME AS RPT. <input type="checkbox"/> OTIC USERS <input type="checkbox"/>			21. ABSTRACT SECURITY CLASSIFICATION UNCLASSIFIED		
22a. NAME OF RESPONSIBLE INDIVIDUAL John J. Larkin			22b. TELEPHONE NUMBER (Include Area Code) (617) 861-5822		22c. OFFICE SYMBOL RADC (ESME)

DD FORM 1473, 83 APR

EDITION OF 1 JAN 73 IS OBSOLETE.

UNCLASSIFIED

SECURITY CLASSIFICATION OF THIS PAGE

TABLE OF CONTENTS

	<u>Page</u>
I. INTRODUCTION.....	1
A. Program Objectives.....	1
B. Background.....	1
C. Approach.....	2
II. LHPG ENGINEERING SUMMARY.....	4
A. LHPG System Configuration.....	4
B. Laser Heating Characterization.....	6
C. Growth of Single Crystal Fibers.....	8
III. MATERIALS SELECTION.....	11
IV. MATERIALS PREPARATION.....	13
A. Feedstock Fabrication.....	13
B. Hot Pressing of Polycrystalline Feedstock.....	13
C. Incorporation of Selected Dopants.....	14
V. CHARACTERIZATION TECHNIQUES.....	15
VI. SINGLE CRYSTAL FIBER GROWTH STUDIES.....	17
A. Oxides.....	17
B. Metastable Materials.....	25
C. Borides, Carbides, and Refractory Metals.....	28
VII. CONCLUSIONS AND RECOMMENDATIONS.....	32
REFERENCES.....	34
FIGURE CAPTIONS.....	35

FINAL TECHNICAL REPORT

I. INTRODUCTION

A. Program Objectives

This report summarizes a 33-month program of research on techniques to grow new and improved quality electromagnetic crystals. The overall objective was to develop the technology to grow single crystal fibers and rods of a variety of materials using the laser-heated pedestal growth (LHPG) method. The study included extensive engineering development of the LHPG crystal growth system; the development of preparative techniques for feedstock; a study of fundamental factors affecting fiber crystal growth; the development of specialized handling techniques for these fibers, because of their small dimensions, to make possible the evaluation of their physical, structural, and chemical properties; and a wide-ranging study of technologically important or otherwise interesting materials selected from a number of classes. Included in this study were materials from the moderate melting oxide class, the refractory oxide class, other high melting compounds such as borides and carbides, metastable materials, and metals. This work was, therefore, in part a feasibility study to evaluate the potential range of application of the LHPG method.

B. Background

The pedestal growth of single crystal fibers is a relatively recent technique which has been made possible by the development of high average power CO₂ lasers. The technique utilizes a differential pulling apparatus and a finely focused laser beam to produce a very small molten "bead" on top of a feed rod, Fig. 1. From this small molten puddle a single crystal fiber of

typical dimensions 50-2000 μm diameter is smoothly and continuously drawn.

The pioneering work in this field was carried out by Haggerty (1), Burrus and Stone (2-4), and Burrus and Coldren (5). The basic technique has a number of unique aspects which give it great versatility. In addition to the high growth speeds made possible by the steep temperature gradients, the technique is containerless, and contamination and stress problems are minimized. Very high temperatures can be achieved with laser-heating, and because only small masses of material are involved, heating and cooling rates are very rapid. The shape of the molten zone, melt convection, macroscopic crystal defects, and the shape of the growth interface in transparent materials, can be observed directly while the crystal is growing.

This program began at a time when the LHPG growth method was first being developed at Stanford University. Our first design was based on the earlier work of Burrus et al., but with the addition of fundamental engineering refinements. During the 33 month duration of this program, and with financial support from both the AFRADC and the NSF/MRL program, the LHPG fiber growth system has been refined, areas of applicability explored, and the truly significant potential of this method as a tool for rapid materials survey and development demonstrated.

C. Approach

The LHPG system was operational in our laboratory approximately one year prior to the beginning of this study. However, consistent with the basic program objectives, the system has remained in a continuous state of engineering modification and upgrading in order to optimize its performance. These activities were therefore dovetailed into the fundamental materials - related studies involving the growth of single crystal fibers and their

The selection of materials ultimately studied evolved during the course of the program. Our initial emphasis was on high-melting materials in the oxide, boride and carbide, and metallic classes; and initial choices included Y_2O_3 , LaB_6 , MgO , TaC , and Nb . These materials were selected to help elucidate problem areas in fiber growth and to help identify the limits of the fiber growth system at the time. Having surveyed these materials, a number of system components were identified as requiring upgrading, and while this work was in progress additional materials were selected for study.

DTIC
ELECTE
MAY 24 1985

OFFICE
OF THE
INSPECTOR
GENERAL

II. LASER-HEATED PEDESTAL GROWTH SYSTEM ENGINEERING SUMMARY

A. LHPG System Configuration

During the course of this study the following LHPG system components were built or added.

1. Microfocus sidearms
2. Microalignment sidearms
3. Atmosphere control chamber
4. Spherical retroreflector
 - a. First generation unit
 - b. Improved second generation unit
5. Laser power attenuator
6. High temperature ceramic chucks
7. Video monitoring system with recorder
8. Hewlett-Packard HP9836 computer
9. Pull and feed platform position encoders
10. Fiber diameter monitoring device by Spectron, Inc.

Details of each of these system engineering modifications can be found in the eight interim reports that were filed. In this final program summary, we describe the system in its final configuration. We also point out the areas where further engineering modifications are required.

A schematic diagram of the LHPG system is shown in Fig. 2. At present a 50 watt CO₂ laser is being used in conjunction with beam-splitting optics to create two opposing beams which are independently adjustable through microalignment and microfocus sidearms. The twin laser beams enter a hermetically sealed atmosphere control chamber through ZnSe windows and intersect on the centerline of the feed and pulling chucks. The source rod, held in the lower chuck can then be fed uniformly upward into the laser beams to create the

molten zone. The hermetically sealed chamber was found to be absolutely essential in preventing stray air currents from causing mechanical perturbations to the growing fiber, and it also allows the use of an inert or reactive atmosphere other than air. It will not, however, permit hard vacuum or elevated pressures. Power to the laser is currently controlled by a three function controller with a 1 Hz bandwidth operating from a thermal detector. Plans to replace this subsystem with a 1 KHz pyroelectric detector/feedback system have been motivated by the desire to improve laser power stability which directly influences fiber diameter uniformity.

We have long felt that some sort of wideband feedback control system would be required to realize optimized fiber diameter uniformity from this type of machine, and look ultimately to a diameter uniformity of $\pm 0.1\%$ in 10-100 μm diameter fibers. Many of the subsystem components which will permit total computerized control of the fiber growth process with a multiloop feedback system have now been obtained. Central to the feedback system is a Hewlett-Packard HP9836 high speed computer which should make possible a 1 KHz bandwidth if the control algorithms are not too complex. The ancillary equipment is identified in the schematic diagram in Fig. 2. The most recent components added are two pull and feed platform position encoders, "Inductosyn" linear tape scale encoders from Farrand Controls with an ± 0.25 micron resolution. At the writing of this report, the position encoders had been bench tested and mounted on the machine but a minor problem with signal conditioning to achieve I/O multiprogrammer compatibility remained to be resolved.

The critical system component, a commercial fiber diameter monitoring system which was contracted from Spectron, Inc., remains as an unresolved item. Bench tests showed that the system performed to its $\pm 0.25 \mu\text{m}$

diameter resolution specifications for an unheated stationary fiber. However, radiant energy from the molten zone during growth caused a number of problems and the machine was returned to the manufacturer for major engineering modifications which have not yet been completed. In the meantime, an alternative fiber "miking" technique having the same resolution has been successfully demonstrated here at Stanford University in the Applied Physics Department. Therefore we now have at least one proven technology as a backup, in addition to the scanning beam technology used in the optical glass fiber industry.

Not shown on the schematic diagram is a video monitoring and recording system which provides a permanent record and an analytical capability for the study of macroscopic stability. In the future this system may also permit measurement of absolute temperatures as well as temperature gradients in the molten zone. A photograph from the video monitor screen demonstrating its surprisingly high resolution of a LiNbO_3 crystal being grown is shown in Fig. 3(a). The crystal growth process is normally monitored through a binocular microscope at magnifications up to 70X. A photograph of the same LiNbO_3 fiber taken directly through the binocular microscope is shown in Fig. 3(b).

The growth station and atmosphere control chamber are shown in Fig. 4(a) and 4(b). The entire system including the laser, growth machine and optical system is mounted on a vibration-damped table. Both fiber and source rod can be rotated in this system. The growth speeds currently available are in the range of 0.025 to 100 mm/min.

B. Laser Heating Characterization

The amount of power necessary to melt a compound depends on its melting point, the diameter of the source rod and the optical absorption

coefficient of the material at $10.6\ \mu\text{m}$. With our 50 watt laser we can easily melt oxide and fluoride compounds up to 2 mm diameter at temperatures as high as 2800°C . These materials absorb $10.6\ \mu\text{m}$ radiation very efficiently. A problem develops, however, when the diameter of the source rod decreases to below approximately $200\ \mu\text{m}$ where less than 1 watt is required to melt even refractory materials such as Al_2O_3 (MP = 2050°C). The relationship between the power necessary to melt three representative oxide compounds as a function of source rod diameter is given in Fig. 5. To rectify this problem, a power attenuator was incorporated into the beam line so that the laser can operate at a stable mid-range power level while at the same time allowing a low output power level to heat the sample.

At the other end of the spectrum are the highly reflecting metals and semiconductors which absorb $10.6\ \mu\text{m}$ but due to their high emissivity, they reradiate the energy with high efficiency. They also have high thermal conductivity losses. These materials cannot be easily melted with a 50 watt CO_2 laser unless the source rod diameter is either very small and/or the material has a low melting point. An internal spherical retroreflector was designed and constructed to fit inside the atmosphere control chamber and minimize molten zone radiation losses. Its use significantly increases process temperatures. The internal spherical retroreflector was constructed by mating two precision hemispherical electroformed reflectors and then machining appropriate holes for the source and seed chucks, the laser beam ports, and the monitoring ports, Fig. 6. Materials such as Si, B_2C , LaB_6 and Nb have been melted with the use of this reflector and small fiber crystals of these materials have been produced. The reflector also diffuses the beam giving more uniform heating of the molten zone. This is an important consideration for materials which undergo a very large change in optical

absorption coefficient when melted. Still, the use of a higher power laser would facilitate the growth of refractory materials with high emissivity.

The image of the growing fiber seen with the spherical retroreflector in place is quite complex because it consists of the object plus an inverted superimposed real image of the same size. It can therefore be quite difficult to achieve and maintain correct alignment during growth. We include a photograph from the video monitor which shows the growth of a sapphire (Al_2O_3) fiber with the spherical retroreflector in place, Fig. 7.

One disadvantage of the two beam optical configuration is that the heating of the molten zone is quite non-uniform. Typical Gaussian beam dimensions are in the 100-200 μm diameter range. Even though the feed rod can be rotated during growth, due to the small masses involved, thermal relaxation times are in the 10's of milliseconds and hot spots cannot be avoided. To circumvent this problem, a new type of optical system was designed by students working under Professor Byer in the Applied Physics Department for use on a second generation specialized LHPG machine. A sectional diagram is included in Fig. 8 and shows the use of a paraboloidal mirror to produce a uniform annular laser beam. The thermal symmetry of the molten zone is greatly enhanced by these newly developed optics. A set of diamond turned optical components has been purchased with partial funding from NSF/MRL and these will be incorporated into our system so that the experimenter will be able to choose between the two types of heating configurations.

C. Growth of Single Crystal Fibers

During normal single crystal fiber growth, the source rod is fed upward until its upper end is melted by the intersecting laser beams. See

of 2.4:1. The fiber obtained displayed the same physical and optical appearance as an undoped LiNbO_3 fiber, but the expected purple color characteristic of the Nd^{+3} ion was not seen. This could have been due to an insufficient amount of Nd incorporated. Assuming no loss of the Nd_2O_3 film applied, a calculation from the Nd_2O_3 film thickness showed that an Nd concentration of 0.13 wt.% should have been incorporated. Absorption and emission spectral analysis are now being carried out to verify the presence of Nd^{+3} and to determine its approximate concentration. Additional growth experiments with higher (1 wt.%) Nd^{+} doping levels are considered highly desirable and will be included in follow-on studies supported through other sources of funding.

7. LiNbO_3 - Ferroelectric Domain Studies

LiNbO_3 is one of the most important electromagnetic materials known. It has a host of applications in acoustics, electro-optics, and non-linear optics. It is particularly important for second harmonic generation and parametric oscillation. Small diameter single crystal fibers will be useful in a number of new fiber optic devices. The growth of LiNbO_3 fibers is relatively straightforward by the LHPG method, and fibers 150-800 μm were grown by both staff and students during this program in lengths up to 6 inches and oriented along both the a- and c-axes.

When bulk crystals of LiNbO_3 are grown by the Czochralski method a series of anti-parallel ferroelectric domains form as the crystals cool through the paraelectric-ferroelectric transition (Curie) temperature a few degrees below the actual melting point. These domains which can be easily revealed by simple polishing and etching techniques (11) can vary in number and morphology depending on melt composition and growth conditions. Various authors (11-14)

of Ti from the molten zone, the concentration of Ti^{3+} in the resulting fiber crystals was found to be very low. A more successful result was achieved by applying a 0.1 wt% titanium metal coating to the surface of a pure sapphire source rod by vacuum evaporation. The titanium was next oxidized to TiO_2 and then a fiber was grown from this material in a reducing Ar atmosphere. The result was a fiber crystal which did have a detectable Ti^{3+} content, although preliminary measurements indicated it was still lower than the levels currently achievable in bulk crystals. These measurements also suggested a somewhat higher broadband absorption than anticipated.

Several alternate approaches exist for increasing the Ti^{3+} dopant concentration. One involves preparing the source rod from hot pressed samples containing a much higher Ti_2O_3 content than found in as-grown crystals. The second involves the application of a much higher amount of sputtered titanium.

A more extensive program on the growth and evaluation of $Ti^{3+}:Al_2O_3$ fiber crystals is underway with follow-on funding from other sources.

6. $LiNbO_3:Nd^{+3}$ - Neodymium doped lithium niobate has been reported to have considerable potential as both a laser host and as an electro-optic material (10). Experiments were undertaken to produce Nd^{3+} doped $LiNbO_3$ single crystal fibers by the same vacuum sputtering dopant application technique used for $Al_2O_3:Ti^{3+}$. A Nd_2O_3 hot pressed pellet was first fabricated for use as a target, and then a 6000 Å layer was sputtered onto one side of a 1.4 mm diameter undoped $LiNbO_3$ source rod.

During fiber growth, the sputtered Nd_2O_3 film appeared to be stable and dissolved in the $LiNbO_3$ melt as the fiber was grown. An oxygen flow rate of 3 lpm was used to keep the film from being reduced or evaporated. The fiber was grown at the normal growth rate of 1 mm/min and the usual diameter reduction

with an 0.9 CO₂/0.1 air ambient for 64 hours. Initial growth experiments employed standard fiber growth parameters, namely a pull rate of 1.0 mm/min and a feed rate of 0.17 mm/min to yield a diameter reduction ratio of a 2.4:1. A static air atmosphere was used and the source rod was rotated at 20 rpm. These fibers, about 700 μm in diameter and 10 cm in length, were among the smoothest and most dimensionally stable of any fiber grown in this system to date, Fig. 13. The first Nb₂O₅ crystals were grown onto the end of a platinum wire and the growth orientation was found to be near the c-axis of its monoclinic unit cell. Along a section of this fiber, twinning was observed, Fig. 14, but the twins were at an angle to the growth direction and grew out soon after formation. Large 1.6 mm diameter rods of Nb₂O₅ were also grown but required a slower growth rate, 0.4 mm/min, and a lower reduction ratio of 1.25:1. For the larger crystals, both the crystal and source rod were rotated.

Proposed studies to introduce selected active ion dopants into this material for study as a laser host were postponed for lack of time.

5. Al₂O₃:Ti³⁺ - An important new crystal for tunable solid state vibronic lasers is Ti³⁺ doped sapphire (9). These crystals have been produced in bulk form with success, but questions still remain concerning the maximum solubility limit of trivalent titanium in Al₂O₃, and how to control the precipitation of TiO₂ and dopant homogeneity.

A series of LHPG fiber growth experiments was therefore undertaken to develop techniques for the growth of fiber crystals of Ti³⁺:Al₂O₃ and to study their properties. In the simplest case, Ti³⁺ doped Al₂O₃ samples cut from bulk crystals grown elsewhere were used as the source material. Due to the small segregation coefficient of Ti³⁺ in Al₂O₃ and perhaps some volatilization

of 2.4:1. The first fiber grown was used as the next feed rod to produce smaller and smaller diameter fibers. The first fibers were unoriented but fibers used as subsequent seeds were oriented at an appropriate angle by the method shown in Fig. 11, using x-ray Laue techniques, to yield new fiber crystals oriented along the a,b and c-axes.

The next challenge was to determine if this compound could be made into a laser crystal by the incorporation of a suitable dopant. Bagdasarov et al. (7) reported on the stimulated emission properties of 5 mm diameter $\text{Nd}^{3+}:\text{CaSc}_2\text{O}_4$ crystals which were presumably grown from the melt, although no details were given. Neodymium-doped CaSc_2O_4 fiber crystals were prepared by the LHPG technique by coating the surface of a hot pressed source rod with a suspension of Nd_2O_3 in toluene by a simple brushing technique. Weighing techniques were used to ascertain the desired 1% Nd^{3+} doping level. During growth the Nd_2O_3 dissolved into the molten zone continuously as the source rod was consumed. This doping technique worked relatively well although a more sophisticated technique, vacuum sputtering, was subsequently developed to achieve better control of the dopant concentration and uniformity.

Digonnet et al. (8) found that $\text{Nd}^{3+}:\text{CaSc}_2\text{O}_4$ fibers produced by this technique lased at $1.05\ \mu\text{m}$ and had the fluorescence spectra at 300°K shown in Fig. 12. While the results in the range of 1.04 to $1.10\ \mu\text{m}$ matched quite well with the data of Bagdasarov et al. (7), the emission observed from 0.85 to $0.95\ \mu\text{m}$ has not been reported before.

4. Nb_2O_5 - The growth of Nb_2O_5 (M.P. = 1495°C) single crystals by any method has not been reported in the literature. The Nb_2O_5 starting material was supplied by IBM Laboratories at Yorktown Heights in the form of hydrostatically pressed bars 2 mm on a side which had been sintered at 1450°C

their optical properties by staff members in the Applied Physics Department.

2. MgO - Only one set of experiments was carried out to grow magnesium oxide (MP = 2800°C) single crystal fibers. Source rods of approximately 1 mm² x 1 cm long were cut from hot pressed material obtained from outside sources. High temperatures were readily achieved in an air ambient and a molten zone achieved. However, an exceedingly high volatilization rate which has been observed by others as well prevented us from achieving a stable melt. X-ray powder diffraction analysis indicated that the starting material was pure. However, we did initiate efforts to obtain single crystal MgO to replace the polycrystalline feedstock. Single crystal feedstock has not, so far, been successfully obtained.

3. CaSc₂O₄ - Calcium scandate, an orthorhombic compound was first reported in 1964 by Carter and Feigelson (6). With only fine polycrystalline samples to work with they used the powder x-ray diffraction method to investigate its crystal structure. Single crystal x-ray analysis would have helped to confirm their results unambiguously, and also permitted a study of its properties. Unfortunately the melting temperature of CaSc₂O₄ is very high, about 2200°C, and so any attempt to prepare single crystals of this material would have been very costly and time consuming. By the LHPG method, members of our staff grew the first single crystals of CaSc₂O₄ in about three hours. Starting with a 20-year old hot pressed sample from which they cut 1 mm square feed rods, clear single crystals in the 100-500 μm range were produced at a growth rate of 1 mm/min. A CaSc₂O₄ fiber is shown in Fig. 10. Only the feed rod was rotated during growth. The ratio of fiber pulling rate to feedstock supply rate was about 6:1 which resulted in a diameter reduction

VI. SINGLE CRYSTAL FIBER GROWTH STUDIES

In this section we summarize the results from all of the various materials studied. In cases where a complete description has been given in one of the interim respects, we refer to that. For materials of greater interest, or where additional data has become available, we include more extensive discussion.

A. Growth of Oxide Materials

1. Y_2O_3 - Yttrium oxide had been grown by the laser-heated pedestal technique before, by J.S. Haggerty (1) in 1972 and by J. Stone and C.A. Burrus (4) in 1977. It was selected here as a model system because of its thermal and physical properties and it was intended to elucidate problem areas in fiber growth rather than as a study of the properties of a particular material. During the third quarter, we concluded our studies on Y_2O_3 (M.P. = 2410°C) which we purposefully doped with Eu_2O_3 . We were able to grow [100] 800 μm diameter rods quite readily using hot-pressed feedstock and an air ambient. Rods grown directly from hot-pressed feedstock tended to fracture after cooling. Haggerty observed similar behavior and attributed the phenomenon to water-enhanced stress corrosion. We also observed rather vigorous gas evolution from this hot-pressed feedstock.

Best results were achieved by using a premelting procedure in which the feedstock was fused by passing the laser beam along the feedstock before growth. Crystal growth at 1.0 mm/min. was then carried out at the usual 2:1 diameter reduction resulting in 800 μm diameter single crystal rods seeded in the [100] direction. The ambient atmosphere used was air, and melts were quiescent with no evidence of gas evolution. During subsequent handling, these Y_2O_3 rods did not fracture. These rods are still being analyzed for

dopants and dopant profiles. DTA and heat treatment procedures were also used for identification purposes.

In the Applied Physics Department single crystal fibers of several materials were fabricated into laser structures and evaluated by lasing performance, laser spectroscopy, and fluorescence methods.

V. CHARACTERIZATION TECHNIQUES

Single crystal fibers were characterized by a number of standard analytical techniques modified somewhat for use on fibers. Because of their small size, fibers present a variety of handling and mounting difficulties. When necessary fibers were encapsulated in acrylic resin or coaxially inside small glass capillaries with low viscosity, low shrink epoxies. If optically flat faces were needed, grooves were sawn into bulk crystals of the same material and the fibers epoxied into these grooves.

Grinding and polishing techniques had to be modified somewhat to minimize edge rounding and breakaway due to differential hardness. Slower polishing rates and finer abrasives usually sufficed. The two sections most commonly prepared were axial (lengthwise) sections, and transverse thin sections. In some cases such as LiNbO_3 fibers, the transverse orientation within the encapsulant had to be maintained so that accurate c-faces or (10.0) faces could be prepared on a-axis fibers. In the particular case of undoped LiNbO_3 fibers, a chemical etching procedure was used in virtually the same manner we would use on macroscopic crystals.

Optical microscopy and SEM were found to be two of the most useful techniques for evaluation of surface, and internal structure in the case of transparent fibers. In thin sections, voids, inclusions, and strain fields were readily apparent as well as the surface pitting on etched LiNbO_3 fibers. See Fig. 9 for an example of cellular structure in a sapphire fiber that was grown in a regime of interface instability.

A host of other analytical techniques were also used for specific situations. X-ray powder diffraction was used to identify phases and structure. Laue XRD was used to orient single crystal fibers for use as seeds. UV fluorescence and electron microprobe analysis were used to study

C. Incorporation of Selected Dopants

Doping can be accomplished by several methods. Dopants can be mixed with the starting powders and then hot pressed or cold pressed and sintered into dense polycrystalline ceramics. If the dopant has a low vapor pressure, a given quantity of dopant can be coated on the surface of the source rod prior to growth. The dopant will then dissolve into the molten zone continuously as the source rod is melted.

A new technique was developed this year for studies where precisely controlled doping levels are required. In this method, the dopant is applied to undoped feedstock bars or rods by vacuum sputtering. In preliminary studies we used a brush-on technique, but found it was difficult to control doping levels. With appropriate heat pretreatment to minimize volatilization of the dopant from the surface of the feedstock before melting temperatures are achieved during growth, we are now able to achieve precise control of dopant levels in materials such as Nd:LiNbO_3 and $\text{Ti:Al}_2\text{O}_3$. Currently, dopants are sputtered onto only one side of a feedstock cylinder. For future laser annealing, solid-state dopant reprofiling, and cladding experiments, a rotating stage inside the vacuum chamber will be constructed to achieve azimuthal uniformity of the sputtered coating.

IV. MATERIALS PREPARATION

A. Feedstock Fabrication

Single crystal, or dense polycrystalline feedstock is the ideal material from which to grow single crystal fibers. A precision micro centerless grinder acquired during the previous year in the Department of Applied Physics is now being used to routinely generate highly uniform cylindrical feedstock. We have used the micro centerless grinder to prepare source rods as small as 300 μm in diameter and 10 cm long, and we are procuring a variable speed motor for the grinder which should allow the grinding of even smaller rods.

When the strength of the bulk feedstock sample is insufficient to allow centerless grinding, we simply prepare square rods of 1 mm dimensions by diamond sawing and grinding. These can be used directly as feedstock, but feedrod rotation is then necessary to achieve uniform melting rates. With cylindrical feedstock, feed rotation is optional.

B. Hot Pressing of Polycrystalline Feedstock

A commercial vacuum hot press (Astro Industries, Inc.) was obtained during the final 18 months of this program with other sources of funding. With the capability of attaining 6000 psi at a temperature of 2000°C using graphite dies, we now have a state-of-the-art capability for fabricating polycrystalline feedstock material from powders. A wide spectrum of doped and undoped oxides, borides, carbides, and silicides is now being hot-pressed into dense discs to support both this program and others.

were discovered somewhat by accident during research on new ferroelectric materials funded by other sources. Only after growing what we thought were their low temperature phases in single crystal fiber form did we discover that we had successfully produced the metastable high temperature phases instead. This was quite an exciting discovery that demonstrated yet another unique capability of the LHPG method.

In Table I, we list a number of representative materials for which some thermophysical properties are known. The two most critical factors which determine how easily and how stably a material can be melted during LHPG are the thermal conductivity and the spectral emittance at both $10.6\text{ }\mu\text{m}$ and in the near IR where the black body curve peaks for temperatures in the 1500°C - 2500°C range. Important too for non-oxides is the possible presence of absorbing surface contaminant films such as SiO_2 on silicon feed rods. In Table II, we list all 14 of the materials studied as part of this program. Detailed descriptions of most of these results are given in a subsequent section.

III. MATERIALS SELECTION

Altogether, a total of 14 materials or material/dopant combinations were studied as part of this program. While it was our initial intention to include studies of eutectic solidification, that work was ultimately carried out with support from other sources, leaving us free to concentrate exclusively on high melting and metastable materials in this study. Research on a number of the materials reported here was carried out with joint funding from other agencies or industrial laboratories and where this was the case, we have so indicated.

Our selection criterion was initially focused on thermophysical properties in order to determine LHPG melting and growth capabilities with the 50 watt CO₂ laser, and to determine the growth characteristics of the different materials classes. It was rather quickly determined that the LHPG system is ideally suited to the growth of oxide materials, and that materials from the other classes such as borides, carbides, and semiconductors tend to be somewhat more difficult due to the physical and optical properties of their molten and solid phases. In certain cases, successful fiber growth could only be accomplished with the use of the spherical retroreflector to reduce radiative heat losses.

Subsequent to these initial survey studies, we added materials which had potential for specific device applications such as Nd:CaSc₂O₄ for a single crystal fiber laser, etc. During this work it became obvious that the study of host/dopant combinations is an area uniquely well-suited to the LHPG method. This is due to its rapid and high crystal quality growth capability, and the ease of adding controlled levels of selected dopants to the feed-stock. Consequently, an increasing emphasis was placed in these areas as the program evolved. The metastable compounds studied near the end of the program

In the LHPG method, molten zone stability was found to be optimum for reduction rates D_s/D_f in the range 1/2 to 1/3 where D_s is the diameter of the source rod and D_f the fiber diameter. To maintain constant diameter one has to keep the melt volume constant through control of the length of zone (L), and ϕ the angle between the crystal and the melt. ϕ is related to the surface tension of the melt and its ability to wet the crystal. Nominally $L = 3(D_s + D_f)/4$.

Unlike the production of glass fibers where the high viscosity of the melt holds the hot zone in alignment, the molten zone of most crystalline materials is of low viscosity and the fiber is free to move if disturbed. Single crystal fiber growth was for this reason found to require a vibration-free environment and one in which air convection is not present. This is the main reason why the chamber was designed and built, although it does have an important secondary advantage of allowing the ambient atmosphere to be varied from reactive to inert. For good diameter control, particularly with the growth of very small diameter fibers on the order of 50 μm or less, excellent mechanical and thermal stability are essential.

Source rods were usually 0.5-1 mm in diameter and smaller diameter fibers were obtained by repetitive growths using the first-grown fiber as the next source rod and so on. Using a 3:1 reduction ratio, a 1 mm starting source rod could be turned into a 37 μm diameter fiber in three growth runs.

To initiate the growth of a single-crystal fiber, a wire, tapered polycrystalline ceramic or single crystal were used for seeding. Single-crystal growth was very easy to achieve with any of these methods. In fact, it was found to be difficult to inhibit single-crystal growth. Crystals were grown along specific crystallographic directions by using oriented seed crystals.

Fig. 1 for reference. A seed is then introduced and the laser power adjusted to maintain a stable molten zone. Growth is initiated by simultaneously starting the pulling and feeding motors. As the fiber starts to grow, the source rod is fed into the laser beam so as to maintain a constant melt volume. In float zone growth the diameter of the crystal and feedstock are the same. In the pedestal growth method the fiber diameter is typically between 1/2 to 1/4 the diameter of the source rod and this is controlled by the ratio of fiber feed to source rod pull rates.

In the schematic shown in Fig. 1 the fiber is being pulled upward which is the method typically used. A few experiments were carried out where we pulled the fibers downward instead. No strong differences were noted, however. The angle of the beam, beam diameter and shape, and laser stability have all been found to be more important factors in determining the shape and stability of the molten zone and the quality of the crystals produced.

Controlled fiber growth requires a stable molten zone. The stability of the molten zone results from a steady-state heat flow at the solid-melt interfaces according to the relationship,

$$Q_s = Q_f + Q_m = A \left(\rho_s \Delta H_f \frac{dx}{dt} + K_l \frac{dT}{dx} \right)_l = A K_s \left(\frac{dT}{dx} \right)_s = \text{Const.}$$

where Q_s is the heat flux in the crystal away from the growth interface, Q_m is the heat flux from the melt toward the interface. Q_f is the latent heat of crystallization, A is the interface area, ρ_s is the density of the solid, ΔH_f is the latent heat, K_l and K_s are the thermal conductivity of the liquid and solid respectively and $(dT/dx)_s$ and $(dT/dx)_l$ are the temperature gradient in the solid and liquid. The shape of the molten zone in pedestal growth is shown in the insert in Fig. 2.

have discussed methods for obtaining single domain crystals and they include applying an electric field during growth, or in an after-growth heat treatment process, or by carefully controlling the growth parameters and impurity concentration in the melt. In practice however, most of the single domain LiNbO_3 crystals produced today are poled after growth by applying an electric field across the c-axis of a grown crystal at a temperature slightly above the Curie temperature.

The domain structure in a ferroelectric single crystal is determined by the requirement that it be in the lowest possible energy state. The total energy (E_T) of such a crystal is the sum of the internal lattice energy (E_I) (affected by internal strain), the domain wall energy (E_W) and the surface energy of the crystal (E_S) i.e.,

$$E_T = E_I + E_W + E_S$$

In large diameter crystals, E_S can be neglected. However, as we reduce the diameter of the crystal to typical fiber dimensions where the surface-to-volume ratio may be several orders of magnitude greater, E_S may have a significant influence on the domain morphology. To determine the influence of E_S on the domain structure, one has to take into account the strain that can be developed in a small diameter fiber under the conditions present during LHPG growth in comparison to the conditions present during large diameter crystal growth by the Czochralski method. Since these factors are currently unknown we were strongly motivated to study ferroelectric domain behavior as a function of growth orientation and fiber diameter.

A study was undertaken to reveal the ferroelectric domain structure in small diameter a- and c-axis LiNbO_3 fibers. This was accomplished by careful

metallographic preparation of cross- and longitudinal-sections followed by chemical etching in 1 HF:2 HNO₃ solution at 90°C for period of approximately 10 minutes. Figure 15(a) shows the domain structure in a c-axis Czochralski-grown boule 1 cm in diameter. In Fig. 15(b), a polished and etched c-axis 700 μ m diameter fiber is shown in which only a small partial skin of antiparallel domain remains surrounding an otherwise single domain crystal. At 500 μ m, LiNbO₃ fibers appear to be completely single domain as shown in Fig. 15(c). These single domain fibers have a strong tendency for growth with the internal polarization directed downward, in parallel with the growth direction. An unexpected finding was the influence of seed polarization on the orientation of c-axis LiNbO₃ fibers. When a single domain seed crystal is used for growth it can be oriented either with the +c or -c facing the melt. It was found that only one of these directions will propagate. If a +c seed is used the fiber crystal will grow with a like polarity. If, however, a -c axis seed is used, the domain orientation will switch so that the +c orientation again faces the melt. The growth ridges in this case do not propagate continuously but rotate by 60° as shown in Fig. 16.

The domain structure in a-axis LiNbO₃ appears to consist of two nose-to-nose antiparallel domains running the entire length of the fiber, Fig. 17. This structure has so far been found in all a-axis fibers under 800 μ m diameter.

A proposed explanation for the ferroelectric domain structure observed in these crystals is that an electric potential is generated near the growth zone by the thermoelectric effect due to the large axial temperature gradients along the c-axis, and that this field is strong enough to orient the domains. This model is consistent with the bipolar domain structures found in a-axis grown crystals, where it is the component of the radial temperature

gradient along the c-axis which creates a plus-minus-plus electric field and leads to the formation of two antiparallel transverse domains.

Initial experiments on poling techniques for a-axis fibers based on direct electric field application and on temperature gradient induced fields were partially successful but did not produce totally single domain fibers. Additional experimentation is needed in this area. The temperature gradient technique is particularly exciting, as it may permit periodic poling, useful for "quasi-phasematched" nonlinear optical interactions.

The dislocation densities observed in the etched LiNbO_3 fibers appear to be quite low. This has led to an interest in studying the influence of dislocations on the optical properties of LiNbO_3 and how the dislocation densities are affected by fiber diameter and growth parameters. Further research would be appropriate in this area as well.

B. Metastable Materials

1. ScTaO_4 - Scandium orthotantalate was originally of interest to us as a novel ferroelectric material. Zhang et al. (15) reported that it has a peak relative permittivity of around 7300 and a Curie temperature of 7°C , which is a convenient temperature for device applications.

At room temperature, scandium tantalate is monoclinic with space group $P2/c$ and lattice constant $a = 4.807 \text{ \AA}$, $b = 5.662 \text{ \AA}$, $c = 5.112 \text{ \AA}$ and $\beta = 91^\circ 37'$ (16). The melting point of ScTaO_4 has been reported by Vladimirova et al. (17) to be 2340°C and it would therefore be difficult to grow single crystals from the melt by conventional techniques. Single crystals were first grown in our laboratory by the flux method of slowly cooling a solution of ScTaO_4 in a $\text{PbO/PbF}_2/\text{B}_2\text{O}_3$ flux from 1250°C . However, their optical and crystal quality was not considered optimum. The laser heated

pedestal growth method was felt to be a particularly suitable alternative for this type of application because of its very high temperature capabilities and since a single crystal fiber can be grown using only a small quantity of starting material. (Scandium compounds at this writing are prohibitively expensive due to their scarcity and newly found application in glass and crystalline laser hosts.)

In these experiments, ScTaO_4 was synthesized from equimolar quantities of Sc_2O_3 and Ta_2O_5 by reactive hot pressing. The samples were mixed by agitation in isopropanol, dried and pressed using the Astro hot press with graphite dies and a hot-pressed boron nitride liner. Samples of about 90% of theoretical density (6.92 g/cm^3) were prepared by pressing for 4 hours at 1350°C under 6000 psi pressure. X-ray diffraction analysis of these samples showed traces of unreacted Ta_2O_5 , so a heat treatment in oxygen at 1200°C for 12 hours was used to complete the reaction. The resulting samples were white and x-ray diffraction showed only the wolframite structure, in agreement with (16).

Single crystal fibers were grown using a laser heater power of 20 W, at a pull rate of 0.5-1 mm/min. Bubbling of the source material was often observed, and was attributed to the presence of carbon from the hot-pressing furnace. Since this bubbling made it difficult to grow a fiber of controlled diameter a two-stage process was normally used in which a fiber of varying diameter was grown in the first stage, and this sample was then regrown to produce a fiber crystal of fairly constant diameter, Fig. 18. The fibers were optically clear and transparent. During growth, it was confirmed by optical pyrometer that ScTaO_4 melts at about 2300°C .

When the single crystal fibers grown by this method were ground and analyzed by x-ray powder diffraction, they were found to be in the tetragonal zircon structure and not the in room temperature wolframite phase. The

tetragonal zircon structure is the stable form of the analogous compound ScVO_4 . The zircon phase in ScTaO_4 had not been reported before and is consequently a new discovery. The lattice parameters of this phase determined by unit cell refinement are $a = 6.786 \text{ \AA}$ and $c = 6.404 \text{ \AA}$ and the powder diffraction data is given in Table III. To verify that the zircon structure was a metastable high temperature phase, single crystal fibers were heated in air to temperatures in excess of 1400°C and held for a period of time. When cooled and again analyzed by XRD, the low temperature wolframite structure was found.

We concluded that because of some characteristic or combination of characteristics unique to the LHPG method, the fibers were able to cool through the phase transition (near 1400°C) without undergoing a phase transformation. Because of the very high temperature gradients involved in LHPG, the transit time through the assumed critical temperature region is probably so short that the phase transition (of first order) cannot occur and the high temperature phase remains "frozen in."

Property measurements on this material will be continued as part of a study on new ferroelectric materials.

2. BaTiO_3 - Like lithium niobate, barium titanate is a very important ferroelectric, acoustic, and optical material. It is difficult to obtain in high quality crystalline form because it undergoes a destructive phase transition at 1460°C and consequently must be grown from TiO_2 solution or a suitable flux. The phase diagram is shown in Fig. 19. Small amounts of strontium substituted for barium are known to stabilize the desired cubic phase all the way to the congruent melting point. Planning ultimately to grow single crystal fibers of the Sr-stabilized cubic phase, we set out to grow

pure BaTiO_3 as a first step. For these experiments, a hot-pressed BaTiO_3 source rod of 2 mm cross section was used. Growth was carried out at a rate of 1 mm/min and a source rotation of 20 rpm was used. Fibers of 800 μm diameter were successfully obtained. As is often the case with polycrystalline feedstock, these fibers were of poor quality and cloudy. However, the result of a subsequent second generation growth down to 300 μm diameter was quite surprising. Transparent, uncracked fibers were obtained, Fig. 20. Yet more surprising was that these fibers were found by x-ray diffraction analysis to be in the metastable high temperature hexagonal phase instead of in the low temperature cubic phase. Using Laue x-ray orientation methods, these fibers were oriented along the optic axis and used as seeds to grow subsequent generations of metastable c-axis fibers, both clear and uncracked.

This is the first time high optical quality, unstrained hexagonal BaTiO_3 has been available for study. This material in single crystal fiber form may have interesting and useful applications and would certainly merit a further determination of its properties.

C. Borides, Carbides, and Refractory Metals

1. LaB_6 - Our first attempts to grow lanthanum hexaboride (M.P. = 2715°C) were unsuccessful due to a lack of sufficient laser power to melt the 0.9 mm² feedstock bar. This result led directly to the fabrication of the first and second generation spherical retroreflectors described in the interim reports. With the retroreflectors a second set of growth experiments, described in the Seventh Quarterly Report was carried out. In these experiments, the atmosphere control chamber was continuously purged with argon gas scrubbed in a hot titanium sponge reactor. One-millimeter hot-pressed LaB_6 source rods obtained from Cerac, Inc. were reduced to 0.5 mm diameter by

centerless OD diamond grinding, and the ceramic chucks described in the interim reports were used.

Melting was achieved and a stable molten zone maintained with approximately 30 W of laser power. Growth was initiated with a pointed Nb wire using pull and feed rates of 1 mm/min. and 0.15 mm/min. respectively, and a source rod rotation of 20 rpm. Growth was initially stable and we were able to grow a fiber about 5 mm long. The fiber obtained appeared to be single and had a diameter in the range of 100-200 μm , Fig. 21. Diameter control in these experiments was poor due to several factors related to both machine parameters and materials parameters. Nonetheless we were able to stably melt and grow LaB_6 as a single crystal fiber.

2. Niobium Metal - Like the case of LaB_6 , our initial attempts to grow niobium (M.P. = 2468°C) single crystal fibers without the use of the spherical retroreflector were unsuccessful. Although we were able to melt a 0.030" feedstock wire, a stable molten zone could not be formed and the molten zone would simply melt its way down the feedwire and out of the hot zone. With the retroreflector in place, a stable molten zone was achieved. Seeding was initiated using a pointed Nb wire. Controlled growth was maintained until the 10 mm long feedwire was totally consumed. The grown fiber appeared to be single-crystal and had a varying diameter in the range of 100 to 200 μm , Fig. 22. The poor diameter control was due mostly to laser power instabilities which are characteristic of our unit when operated near maximum power output in a manually-controlled open-loop mode. Minor variations in the diameter of the feedwire were also present.

These experiments represented the first time a stable molten zone of niobium metal had been achieved in our fiber growth apparatus. The mechanism

by which the spherical retroreflector stabilized the niobium molten zone, however is still not understood in view of our earlier experience with Nb melts.

3. B₉C - Boron carbides are of interest primarily as hard refractory semiconductors and they may also have potential as high temperature thermoelectric materials. The boron-carbon system shows a continuous range of solid solutions from B₄C to B_{10.5}C (18) with the rhombohedral B₄C structure, which is closely related to that of α -boron. The liquidus temperature varies slowly throughout this range and has a maximum of 2460°C at a composition near to B₅C. The known phase equilibrium in the partial B-C system is shown in Fig. 23. All compositions probably melt incongruently but the difference between liquidus and solidus temperature is small. Single crystals are essential to gain a better understanding of the fundamental electrical conduction mechanism in these materials. It is difficult to obtain useful crystals of these materials by any technique.

We carried out growth experiments on two compositions, B_{6.5}C and B₉C, which are the most favorable for thermoelectric applications. Cylindrical rods 0.5-1 mm in diameter were machined from hot pressed samples to provide the source material. It was found to be very difficult to melt this material without the use of the retroreflecting sphere. Even with the first generation sphere, it was found difficult to maintain a stable molten zone. The melts tended to migrate under gravity and solidify with radial processes. The best sample produced was about 2 mm long and 300 μ m in diameter, Fig. 24. It has a very irregular surface but is larger than any other crystals of this material that have been reported from chemical vapor transport methods.

Electrical conductivity measurements will be made on this crystal as part of our continuing study of basic materials properties. In light of our success, subsequent growth experiments seem warranted now that we have the improved second generation spherical retroreflector operational.

VII. CONCLUSIONS AND RECOMMENDATIONS

At the end of this 33 month research program a number of conclusions and observations can be made. The program has been outstandingly successful from our point of view by having made it possible to develop and to define the range of application of the LHPG method. The diversity of this program has allowed us to carry out major engineering development of the LHPG apparatus, as well as to study a broad range of materials representing a variety of growth related problems. The desire to determine the ferroelectric domain structure in LiNbO_3 fibers has led to the development of preparation and etching techniques that have not previously been applied to single crystal fiber structures.

We have clearly demonstrated that the LHPG technique can be used to grow single crystal fibers of high melting materials, including oxides, borides and carbides, and metals, as long as their melts do not decompose or sublime too rapidly. Growth from high temperature solutions, as in the case of SiB_6 , were not carried out but can be anticipated to be very sensitive to molten zone, temperature, and growth rate stability.

Fiber diameter uniformity and ease of growth were found to be distinctly different for the oxides compared with the non-oxide materials studied, with the oxides being substantially easier to grow. Several reasons for this were determined: oxides readily absorb $10.6 \mu\text{m}$ radiation and they lose heat only moderately by conductive and radiative mechanisms. In contrast, the non-oxides tend to have substantially higher conductive and radiative heat losses making them much more difficult to melt stably. The use of a retroreflecting sphere was shown to mitigate the problem to a degree.

There can be no doubt that the LHPG method will have a major impact on the development of new optical materials. We have demonstrated the ease of

single crystal fiber preparation combined with the ability to introduce precisely controlled levels of specific dopants. This technology will rapid speed the development of new optical host/dopant combinations. It should also enhance the field of predictive methodology by making verification significantly easier. It is our opinion that the ease of materials preparation by this method can far outstrip our ability to adequately characterize these fibers using current techniques. Single crystal fibers because they are small, are difficult to handle. Major improvements in small scale characterization technology will therefore be needed in order to make optimum use of the LHPG method.

Specific applications for non-oxides such as LaB_6 which can be grown directly in fiber form for use as filamentary electron emitters can also be envisioned. The pedestal growth method is certainly well-suited to this application. However, less costly alternative means for establishing the molten zone such as by electron beam heating should be explored.

Finally, we have discovered the relative ease of producing single crystal fibers of metastable high temperature phases by the LHPG method. We thus have available in fiber form a range of new single crystal materials that are not readily obtainable by other methods. Measurements of physical properties and doping studies will be needed in order to identify possible applications for them.

REFERENCES

- (1) J.S. Haggerty, "Production of Fibers by a Floating Zone Fiber Drawing Technique," Final Report NASA-CR-120948, May 1972.
- (2) C.A. Burrus and J. Stone, Appl. Phys. Lett., 26, 318 (1975).
- (3) J. Stone, C.A. Burrus, A.G. Dentai and B.I. Miller, Appl. Phys. Lett., 29, 37 (1976).
- (4) J. Stone, C.A. Burrus, J. Appl. Phys., 49, 2281 (1978).
- (5) C. A. Burrus and L.A. Coldren, Appl. Phys. Lett., 31, 383 (1977).
- (6) J.R. Carter and R.S. Feigelson, J. Amer. Ceramic Soc., 47, 141 (1964).
- (7) Kh. S. Bagdasarov, A.A. Kaminsicii, A.M. Kevorkov, and A.M. Prokhorov, Soviet J. Quant. Electron, 4, 927 (1975).
- (8) M.J. Digonnet, H.J. Shaw, W.L. Kway and R.S. Feigelson, unpublished.
- (9) P. Moulten, Optics News 9, (1982).
- (10) Review article in Laser Crystals, Ed. A.A. Kaminskii.
- (11) K. Nassau, H.J. Levinstein and G.M. Loiacono, Appl. Phys. Lett. 6, 228 (1965).
- (12) H.T. Parfitt and D.S. Robertson, Brit. J. Appl. Phys., 18, 1709 (1967).
- (13) K.G. Deshmukh and K. Singh, J. Phys. D: Appl. Phys. 5, 1680 (1972).
- (14) N. Niizeki, T. Yamada and H. Toyoda, Jap. J. Appl. Phys. 6, 318 (1967).
- (15) W.L. Zhong, P.L. Zhang, and H.C. Chen, Solid State Comm. 49, 467 (1984).
- (16) ASTM Index, Card 24-1017 (McIlv Reid and McCarthy, Penn State Univ., 1972).
- (17) Z.A. Vladimirova, V.K. Trunov, L.N. Komissarova, Russ. J. Inorg. Chem., 15, 1491 (1970).
- (18) M. Bouchacourt and F. Thevenot, J. Less Common Metals 82, 227 (1981).
- (19) G.V. Samsonov and I.M. Vinitiskii, Handbook of Refractory Compounds. Plenum Press, p. 525 (1980).

TABLE I

MATERIAL	M.P. (PERITECTIC DECOMPOSITION)	THERMAL CONDUCTIVITY AT M.P. (AT 300°K)	EMITTANCE EXTRAPOLATED TO M.P.	ELECTRONIC CHARACTERISTICS
Y_2O_3	2410°C	0.05-0.1 W/cm ² C	Total Normal = 0.3-0.5 Normal Spectral at 10.6 μ m = 0.9-1.0	Insulator
LaB_6	2715°C	0.34	Normal Spectral at 0.65 μ m = 0.7-0.8	Metallic
MgO	2800°C	0.02-0.04	Total Normal = 0.9	Insulator
TaC	3880°C	0.6	Hemispherical Total = 0.5-0.6	Metallic
Nb	2468°C	0.9-1.0	Hemispherical Total = 0.3 Normal Spectral at 10.6 μ m = 0.1-0.2	Metallic
SiB_6	(1900°C)	0.1	--	Semiconductor
Si	1410°C	(2.0)	(No High Temperature Data Found)	Semiconductor
Nb_2O_5	1495°C	NA	Normal Spectral at 1000°C E = 0.2 @ 1.0 μ m, E = 0.9 @ 10 μ m	Insulator
$LiNbO_3$	1260°C	--	--	Insulator
Al_2O_3	2045°C	0.2	Total Normal = 0.3-0.45	Insulator
YAG	1900°C	0.04	--	Insulator

Majority of data from "Thermophysical Properties of Matter," Ed. Y. S. Touloukian, Plenum Publishing Co. (1970)

Material	M.P.	Fiber Diameters		Atmospheres	Spherical Retroreflector	Results
		Grown	Drawn			
$Y_2O_3:Eu$	2410°C	800 μm		Air	No	High optical quality fibers grown at slow growth rates to avoid thermal shock and cracking.
LaB_6	2715°C	200 μm		Argon	Yes	Single crystal fiber successfully grown using retroreflector. Power fluctuations caused diameter non-uniformity.
Ag	2800°C	N/A		Air	No	Excessive sublimation rate prevented stable growth.
TaC	3880°C	N/A		Argon	—	—
Nb	2468°C	200 μm		Argon	Yes	Single crystal fiber successfully grown using retroreflector. Power fluctuations and feedwire variations contributed to diameter variations.
$CaSc_2O_4$	2110°C	600 μm		Air	No	First single crystal ever grown from the melt. Oriented fibers grown from fiber seed.
$CaSc_2O_4:Ni^{+3}$	2110°C	600 μm		Air	No	High optical quality doped crystal using brush-on application technique. Fluorescence and lasing demonstrated.
Nb_2O_5	1495°C	1700 μm		O ₂	No	Comparatively large diameter high optical quality crystal readily produced by regrowth technique using both seed and source rotation.
$LiNbO_3$	1260°C	800-300 μm		Air	No	a-axis and c-axis fibers grown for first ever studies on ferroelectric domain structure in fibers.
$LiNbO_3:Ni$	1260°C	800 μm		Air	No	Vacuum sputtering technique successfully used to introduce controlled dopant levels in high optical quality fibers.
$Al_2O_3:Ti^{+3}$	2045°C	800 μm		Argon	Yes	Ti^{+3} successfully incorporated but at lower concentration than planned due to volatilization of dopant. Control of valence state by reactive atmosphere processing highly successful.
$BaTiO_3$ [Hex. Phase]	1618°C	800 μm		Air	No	High optical quality oriented single crystal fibers of high-temperature metastable hexagonal phase. First time produced without quenching.
$ScTaO_4$ [Zircon Phase]	2300°C	800-300 μm		Air	No	Regrowth technique successful in producing high optical and structured quality crystal fiber from minimal amount of scarce material. As a bonus, previously unknown high temperature metastable zircon phase discovered.
B_2O_3	2400°C	200 μm		Argon	Yes	Successful single crystal fiber growth using spherical retroreflector. Very difficult by other methods.

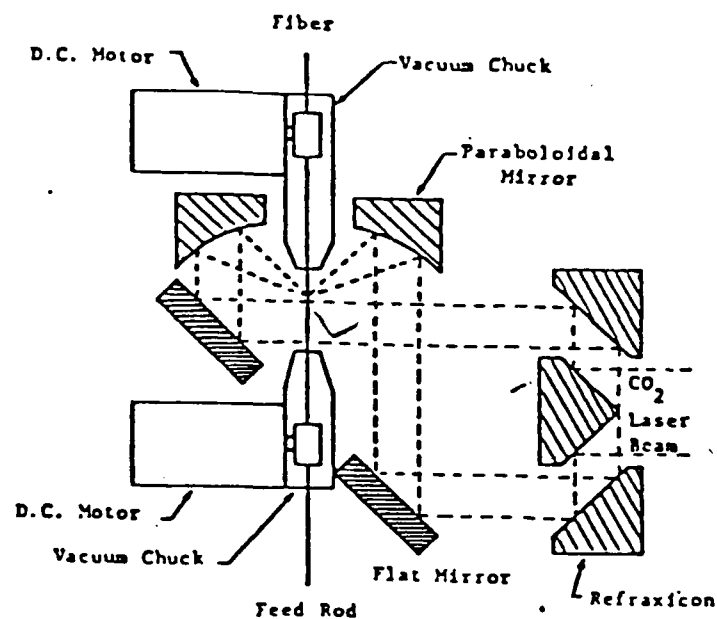


Fig. 8 Schematic of the axially symmetric optic system designed to provide uniform 360° illumination of the molten zone.

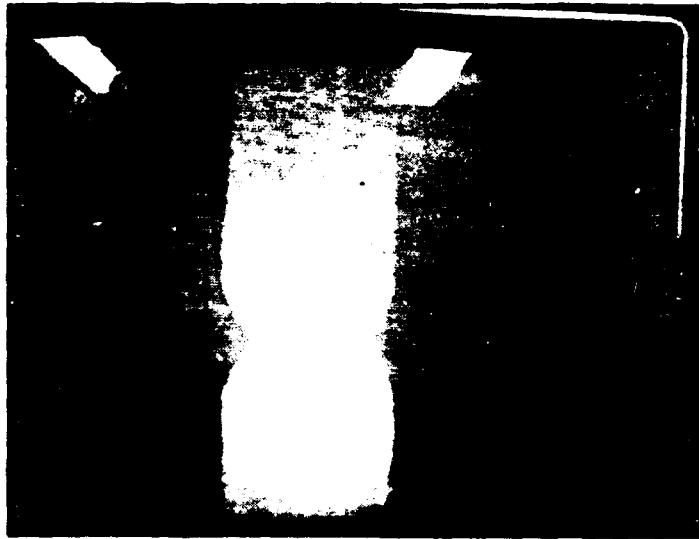


Fig. 7 Photograph from video monitor of a sapphire fiber being grown with the aid of the spherical retroreflector. The inverted image superimposed on the object is a consequence of the molten zone being positioned at the focus of the spherical cavity. Radiative losses are reduced by 70% with the sphere, and higher melt temperature can be achieved.



Fig. 6 Second generation spherical retroreflector which has a tighter focus due to improved relative alignment of the two hemispherical irros.

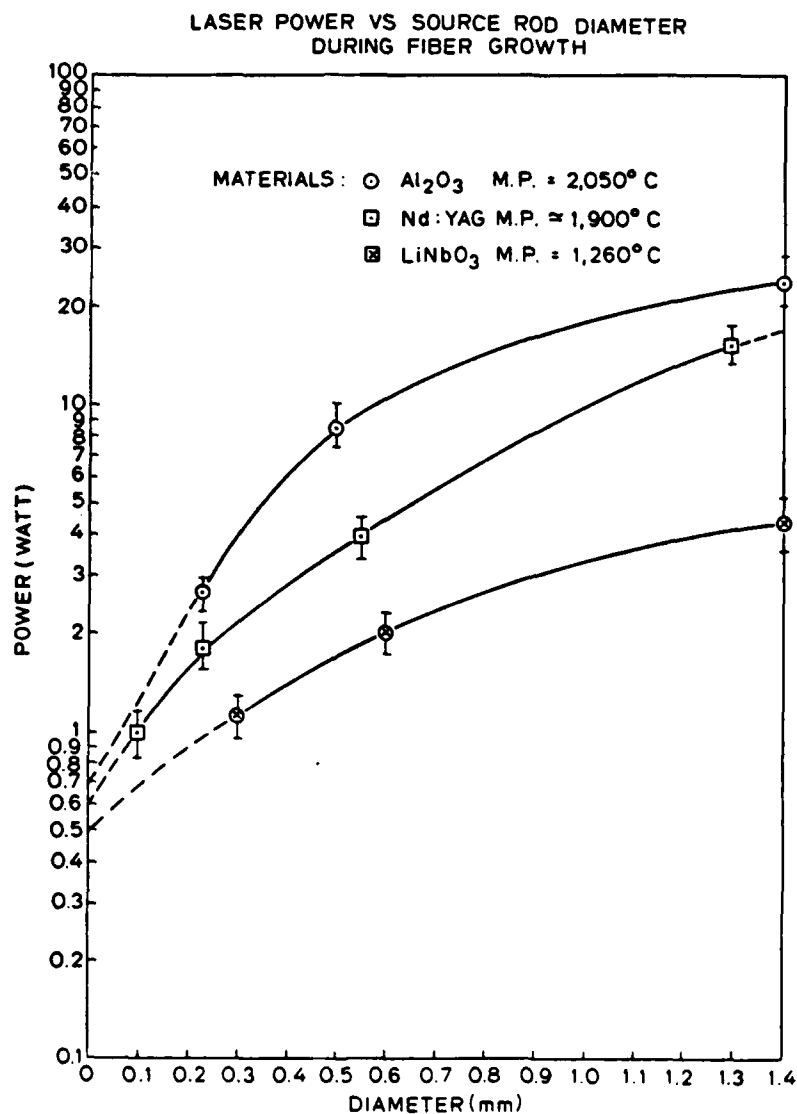


Fig. 5 The CO_2 laser power necessary to form a molten zone in Al_2O_3 , Nd:YAG, and LiNbO_3 as a function of source rod diameter.

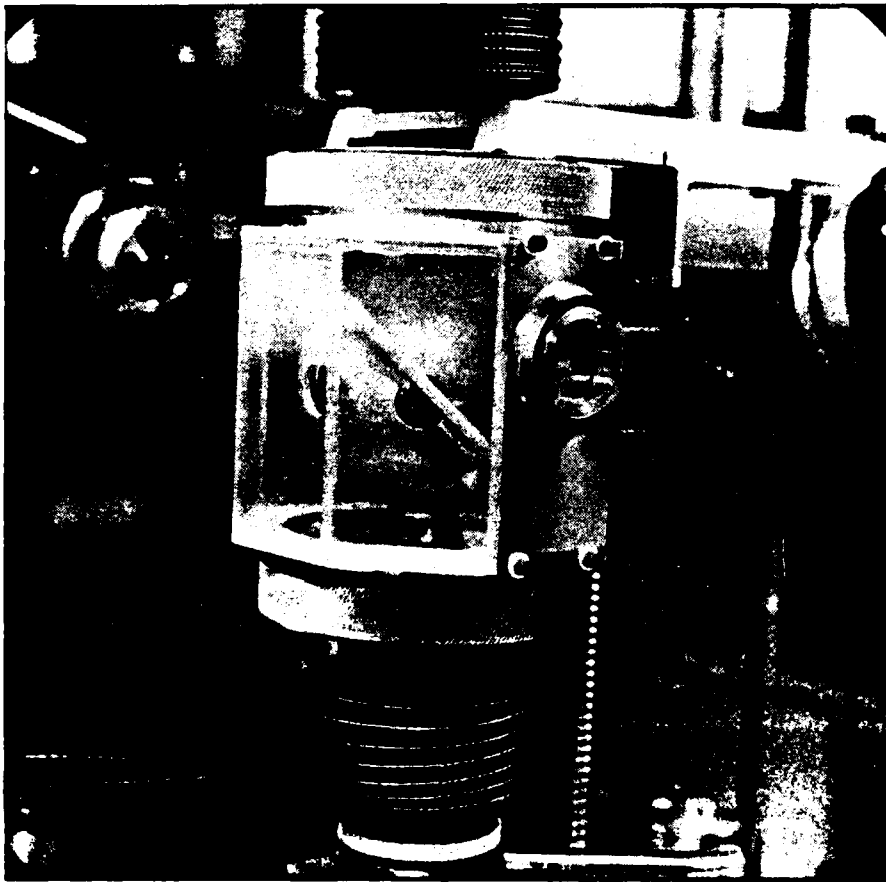


Fig. 4b Atmosphere control chamber with first generation retroreflector in place.

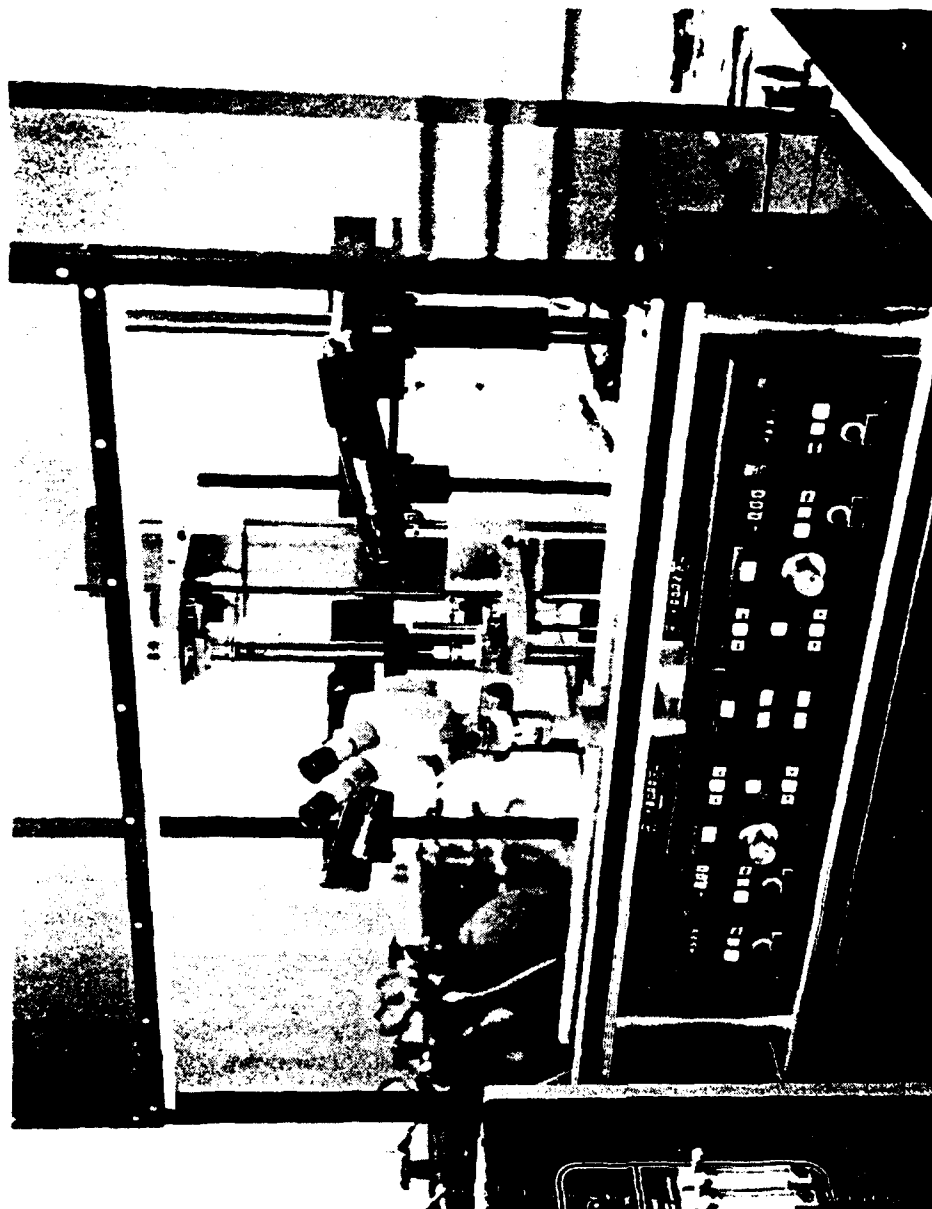
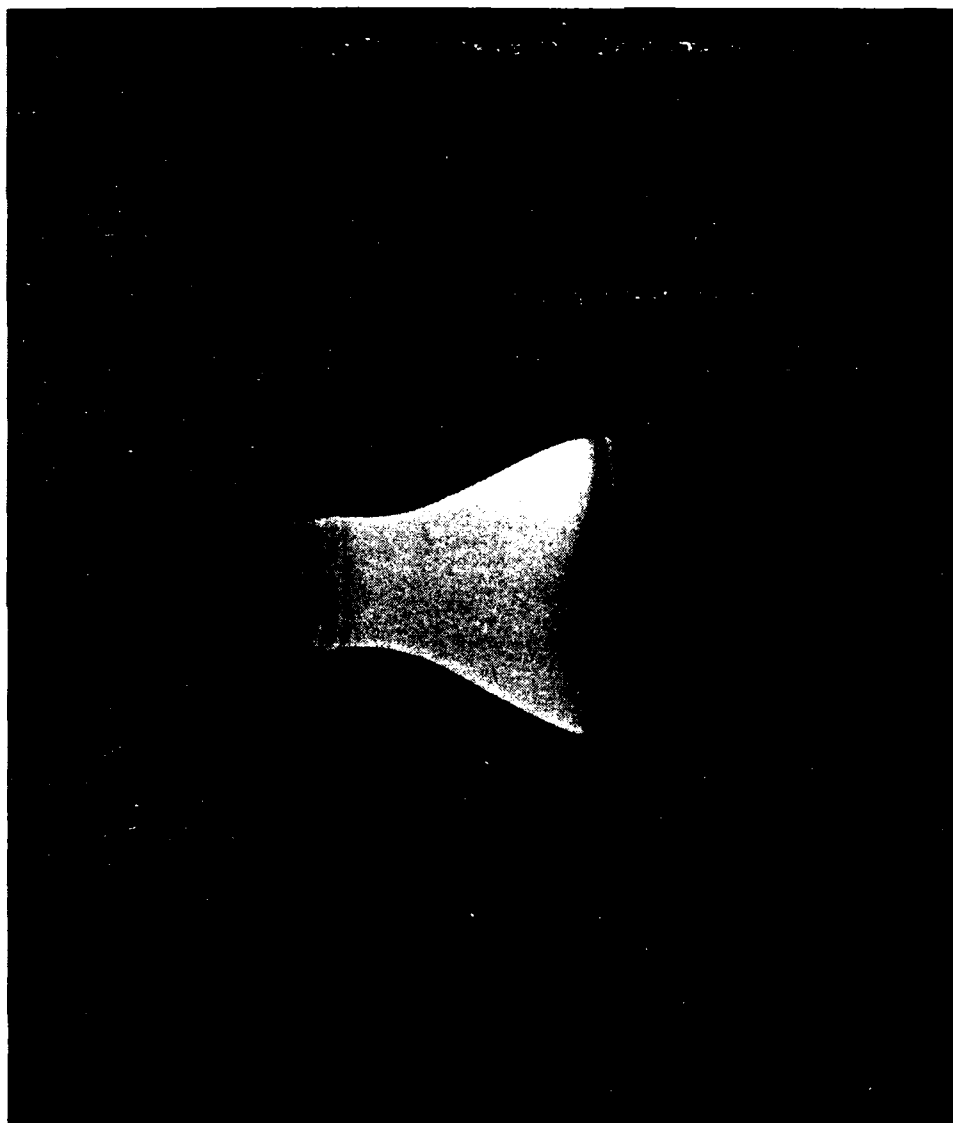
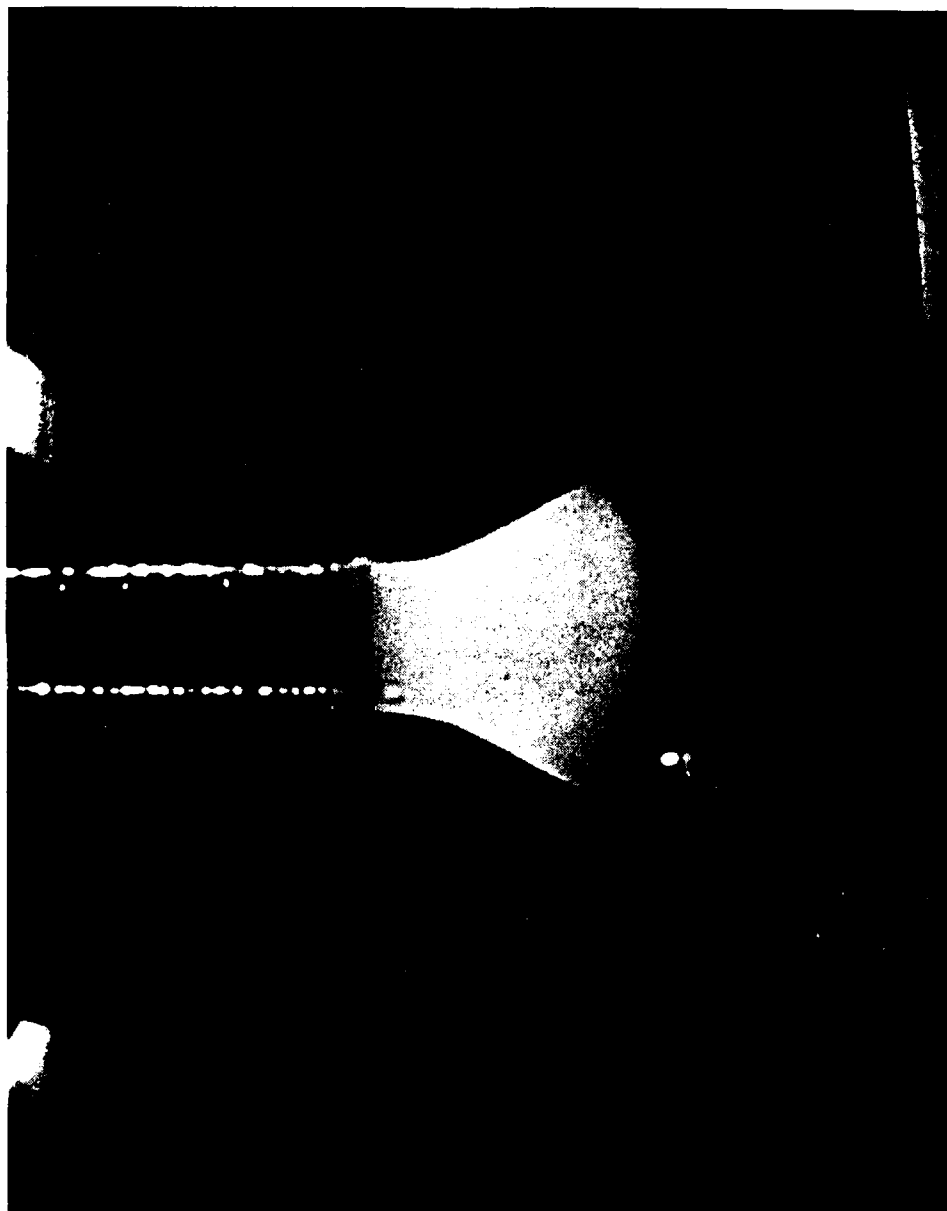


Fig. 4a Photograph of the growth station mounted on vibration-damped table. Laser sidearms, viewing microscope, and pulling mechanism are visible.



3(b)



3(a)

Fig. 3 Photograph of a LiNbO_3 Single crystal fiber being grown (a) from a video monitor, and (b) directly through binocular microscope. The feedstock was a centerless-ground bulk crystal rod.

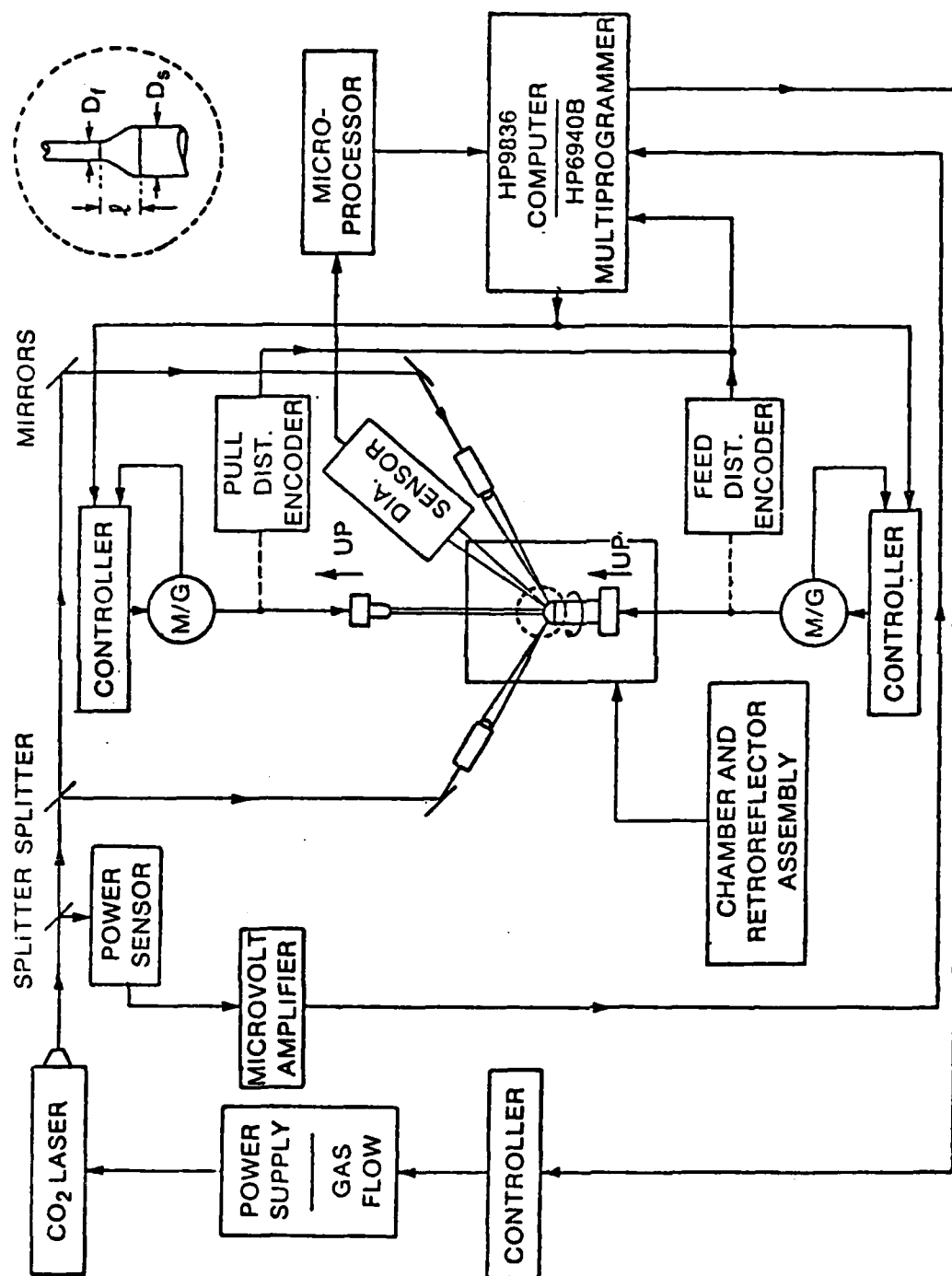


Fig. 2 Schematic of the two-beam laser heated pedestal growth apparatus showing major components and the planned feedback loops. All components except the diameter sensor have now been assembled and are being integrated into the system.

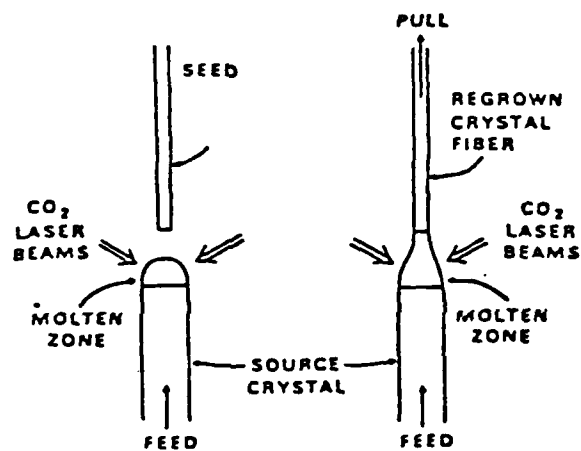


Fig. 1 Schematic of the pedestal growth technique with CO₂ laser heating. In this configuration the growing fiber is pulled upward out of the molten zone. The process can equally well be inverted and the fiber pulled down.

18. Optical micrograph of a ScTaO_4 fiber, all of which have been found to be in the high temperature metastable zircon phase which has tetragonal (4/mmm) symmetry.
19. Partial phase diagram of the BaO-TiO_2 system after D.E. Rase and R. Roy, J. Am. Ceramic Soc. 38, 110 (1955). In equilibrium, above 1460°C , BaTiO_3 is found in the hexagonal non-ferroelectric phase.
20. Optical micrograph of a metastable hexagonal BaTiO_3 single crystal fiber grown from a hot-pressed polycrystalline source rod.
21. First LaB_6 single crystal fiber grown with the initial spherical retro-reflector in place. Laser power fluctuations caused diameter variations.
22. Scanning electron micrograph of the first niobium metal single crystal fiber grown from a 0.030" diameter feedwire. Laser power fluctuations again caused diameter variations.
23. Partial phase diagram of the B-C system showing the broad existence region of the rhombohedral B_4C -type phase, after G.V. Samsonov and I.M. Vinitskii, from Handbook of Refractory Materials, Plenum Press (1980), p. 525.
24. Scanning electron micrograph composite of the first B_9C single crystal to be grown from the melt by any technique.

9. Cellular structure in a sapphire fiber grown at 40 mm/min (150X).
10. A single crystal fiber of CaSc_2O_4 grown along the a-axis by the LHPG method.
11. Photograph illustrating the method by which randomly nucleated single crystals are first Laue oriented and then held along major crystallographic axes for use as oriented seeds.
12. Fluorescence spectra of a Nd^{+3} doped CaSc_2O_4 crystal.
13. Scanning electron micrograph of a 700 μm diameter single crystal of Nb_2O_5 grown in an air ambient from a hot-pressed polycrystalline bar. Minor growth ridges are apparent, but otherwise this fiber was among the smoothest and most dimensionally stable that have been grown.
14. Section of randomly nucleated Nb_2O_5 fiber showing twin bands which formed at a shallow angle to the growth direction and eventually grew out.
15. As-grown ferroelectric domain structure in LiNbO_3 crystals. (a) Cross section of 1 cm, c-axis Czochralski boule showing concentric rings. (b) Cross-section of 700 μm , c-axis single crystal fiber where only a small partial skin of an antiparallel domain can be seen. (c) At 500 μm diameter and below LiNbO_3 fibers are totally single-domain as grown.
16. The effect of c-axis seed polarity on the growth of LiNbO_3 single domain fibers. If we attempt to grow with a seed of opposite polarity to the preferred positive direction facing the melt, the growing fiber undergoes an inversion with the consequence that the 3-fold growth ridges appear to rotate by 60° .
17. Longitudinal section showing the (10.0) plane of an a-axis LiNbO_3 fiber. Etching has revealed a bipolar nose-to-nose domain structure along the entire length of the fiber.

FIGURE CAPTIONS

1. Schematic of the pedestal growth technique with CO_2 laser heating. In this configuration the growing fiber is pulled upward out of the molten zone. The process can equally well be inverted and the fiber pulled down.
2. Schematic of the two-beam laser heated pedestal growth apparatus showing major components and the planned feedback loops. All components except the diameter sensor have now been assembled and are being integrated into the system.
3. Photograph of a LiNbO_3 single crystal fiber being grown (a) from video monitor, and (b) directly through binocular microscope. The feedstock was a centerless-ground bulk crystal rod.
4. (a) Photograph of the growth station mounted on vibration-damped table. Laser sidearms, viewing microscope, and pulling mechanism are visible. (b) Atmosphere control chamber with first generation retro-reflector in place.
5. The CO_2 laser power necessary to form a molten zone in Al_2O_3 , Nd:YAG, and LiNbO_3 as a function of source rod diameter.
6. Second generation spherical retroreflector which has a tighter focus due to improved relative alignment of the two hemispherical mirrors.
7. Photograph from video monitor of a sapphire fiber being grown with the aid of the spherical retroreflector. The inverted image superimposed on the object is a consequence of the molten zone being positioned at the focus of the spherical cavity. Radiative losses are reduced by 70% with the sphere, and higher melt temperatures can be achieved.
8. Schematic of the axially symmetric optic system designed to provide uniform 360° illumination of the molten zone.

TABLE III

Scandium Tantalate XRD Data

Tetragonal I 4/amd

$$a = 6.78653 \pm .04258$$

$$c = 6.40388 \pm .04343$$

<u>hkl</u>	<u>T(%)</u>	<u>d(Å)</u>
020	100	3.394
112	43	2.663
220	42	2.399
022	3	2.329
130	5	2.146
132	93	1.7827
040	36	1.697
240	44	1.518
024	8	1.4479
332	10	1.431
224	6	1.332
152	13	1.229
440	3	1.1997
044	4	1.1644
060	11	1.1313
244	14	1.1014
352	19	1.0939
260	20	1.0731
444	7	1.0218



Fig. 9 Cellular structure in a sapphire fiber grown at 40 mm/min (150x).

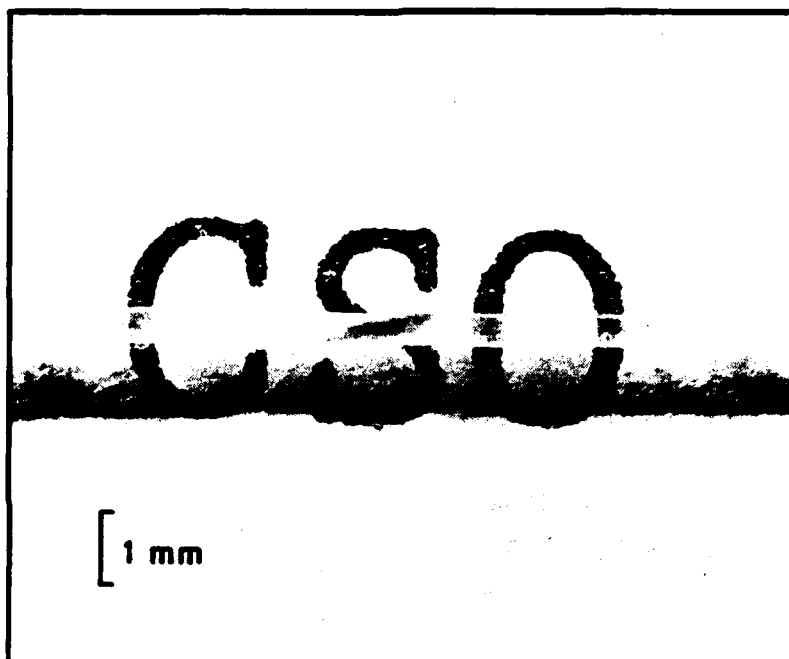


Fig. 10 A single crystal fiber of CaSc_2O_4 grown along the a -axis by the LHPG method.

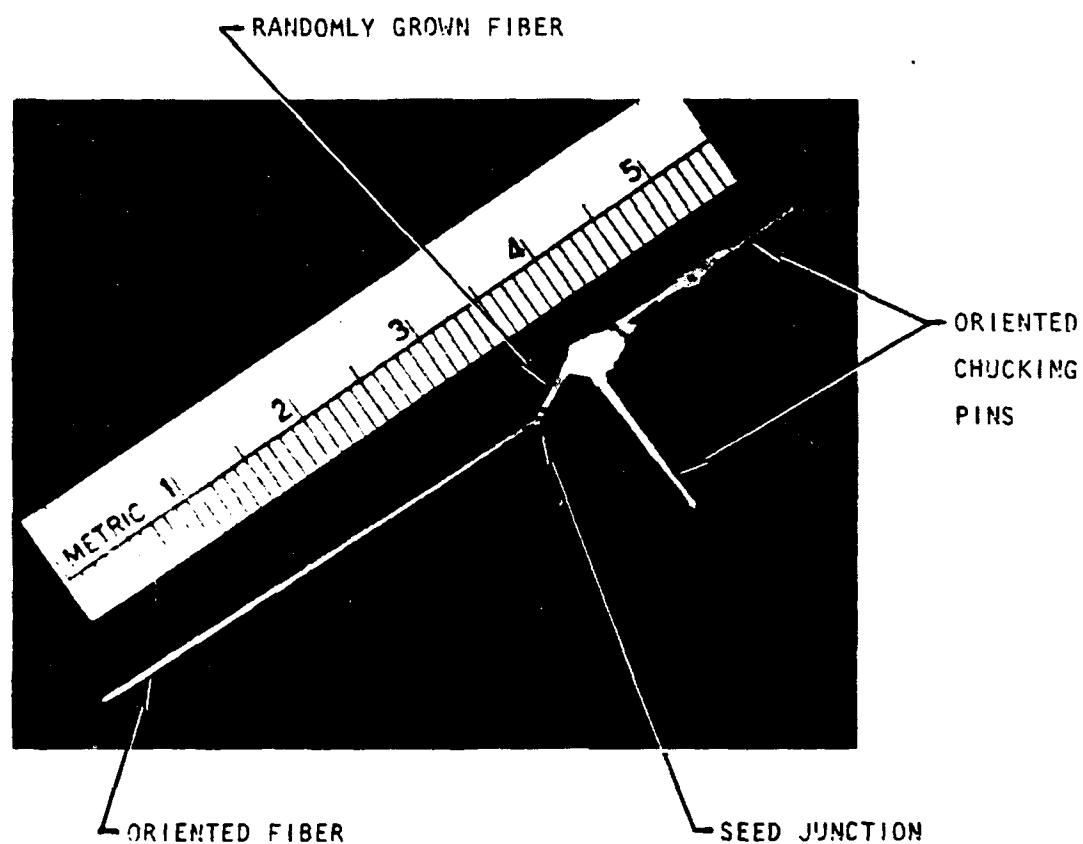


Fig. 11 Photograph illustrating the method by which randomly nucleated single crystals are first Laue oriented and then held along major crystallographic axes for use as oriented seeds.

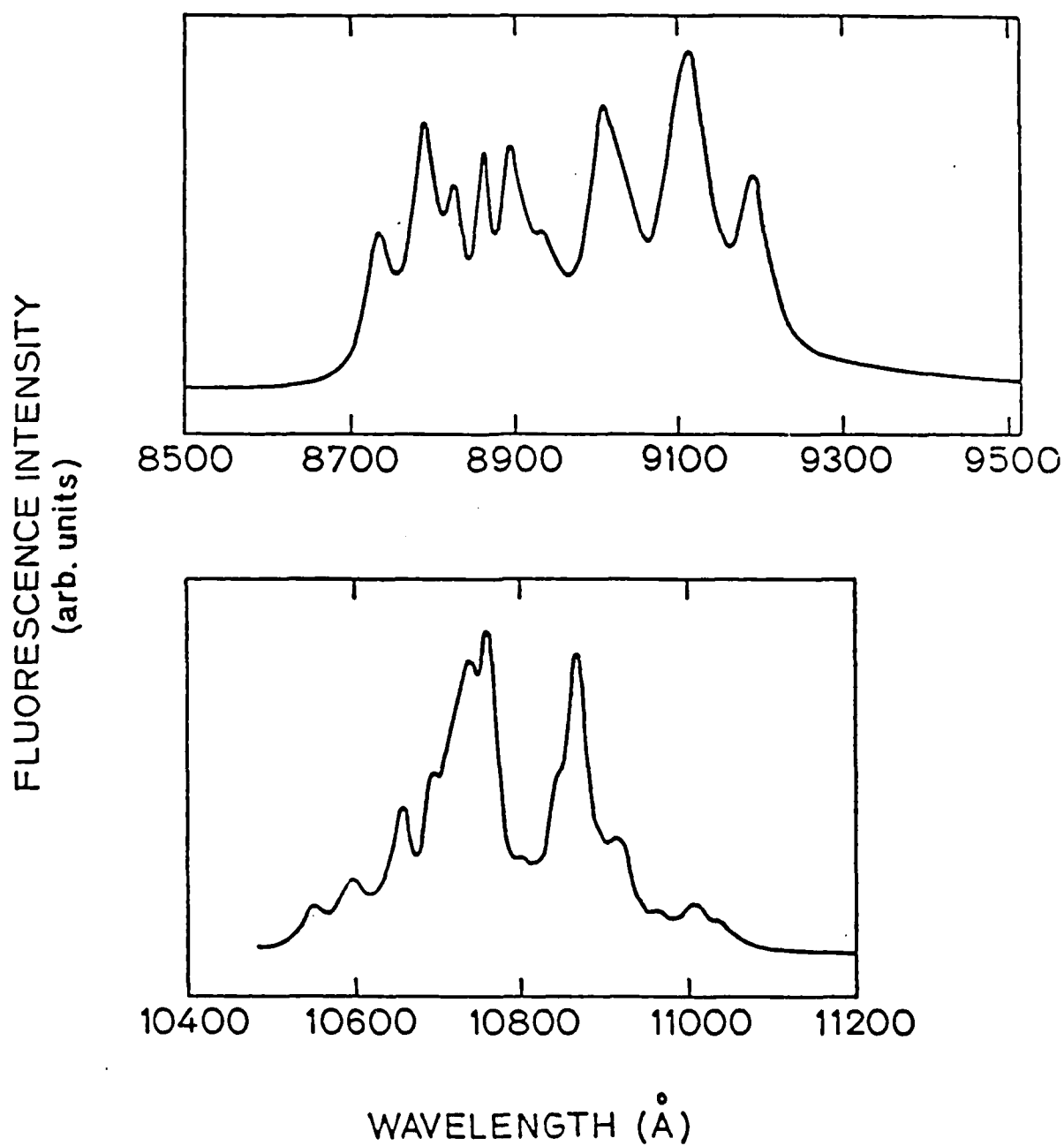


Fig. 12 Fluorescence spectra of a Nd^{+3} doped CaSc_2O_4 crystal.

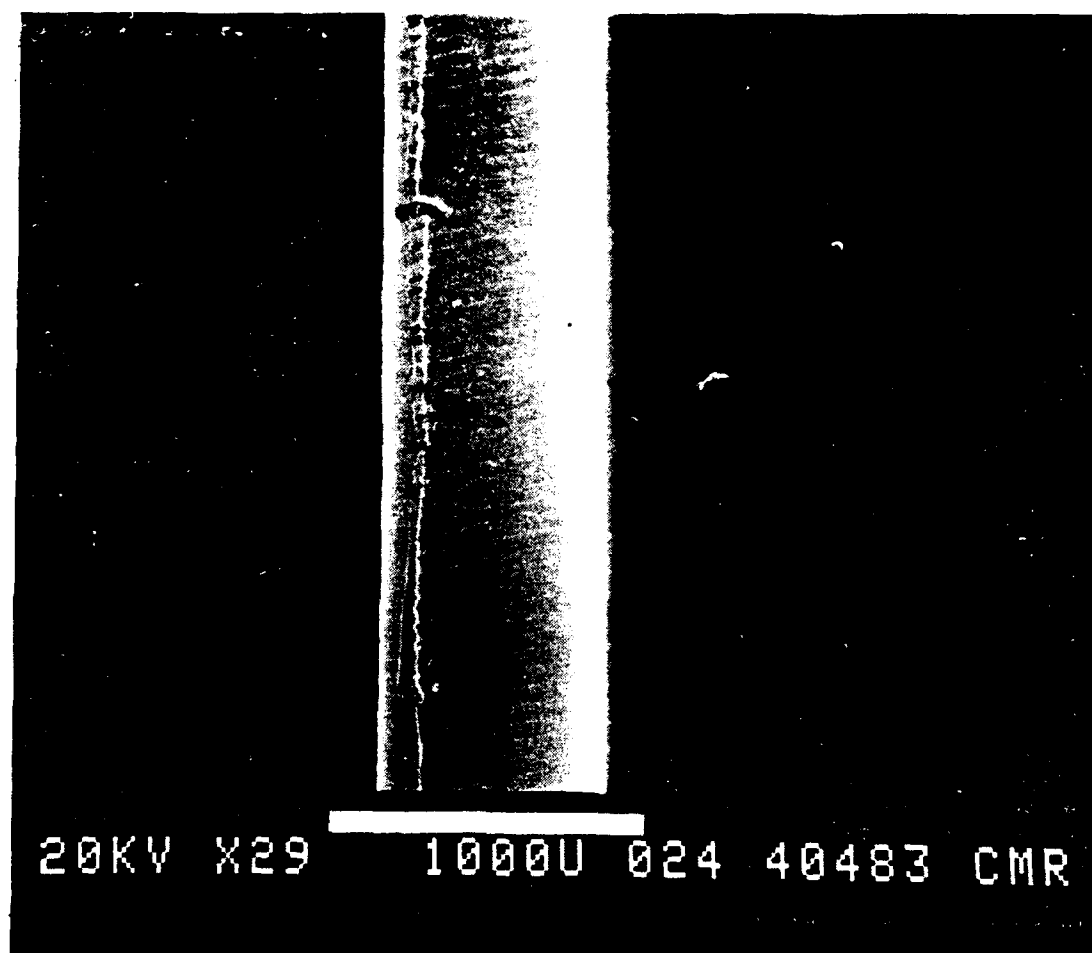


Fig. 13 Scanning electron micrograph of a 700 μ m diameter single crystal of Nb₂O₅ grown in an air ambient from a hot-pressed polycrystalline bar. Minor growth ridges are apparent, but otherwise this fiber was among the smoothest and most dimensionally stable that have been grown.

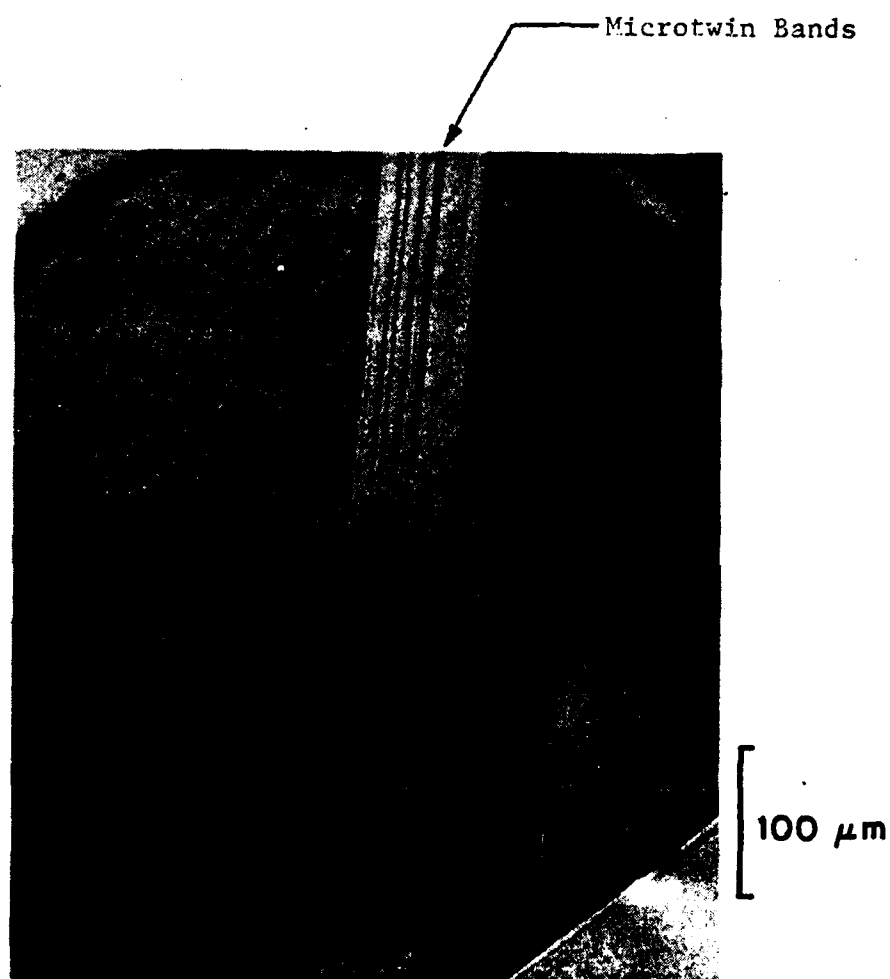


Fig. 14 Section of randomly nucleated Nb_2O_5 fiber showing twin bands which formed at a shallow angle to the growth direction and eventually grew out.

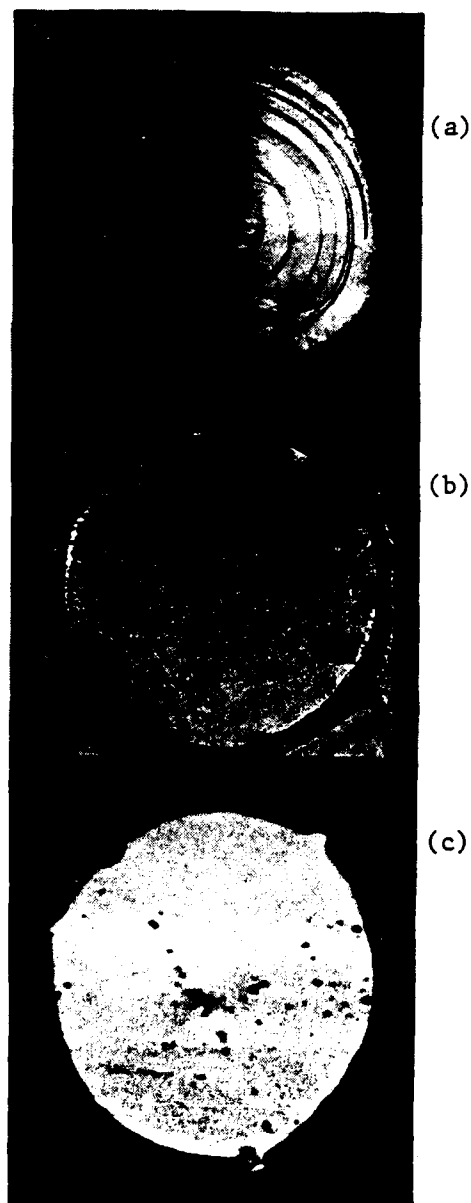


Fig. 15 As-grown ferroelectric domain structure in LiNbO_3 crystals.
 (a) Cross-section of 1 cm, c-axis Czochralski boule showing concentric rings. (b) Cross-section of 700 μm , c-axis single crystal fiber where only a small partial skin of an antiparallel domain can be seen.
 (c) At 500 μm diameter and below LiNbO_3 fibers are totally single-domain as grown.

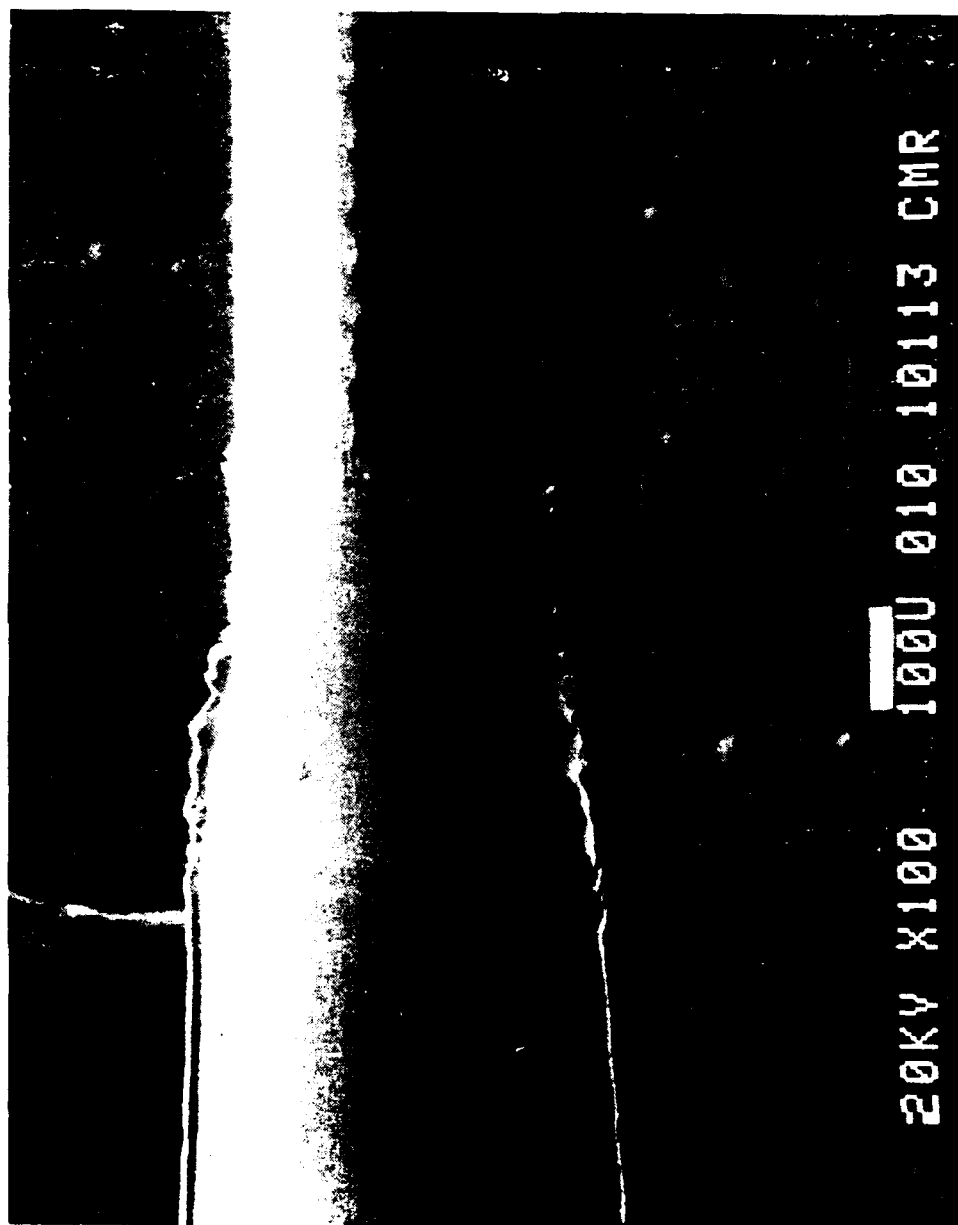


Fig. 16 The effect of c-axis seed polarity on the growth of LiNbO_3 single domain fibers. If one attempts to grow with a seed of opposite polarity to the preferred positive direction facing the melt, the growing fiber undergoes an inversion with the consequence that the 3-fold growth ridges appear to rotate by 60° .



Fig. 17 Longitudinal section showing the (10.0) plane of an a-axis LiNbO_3 fiber. Etching has revealed a bipolar nose-to-nose domain structure along the entire length of the fiber.

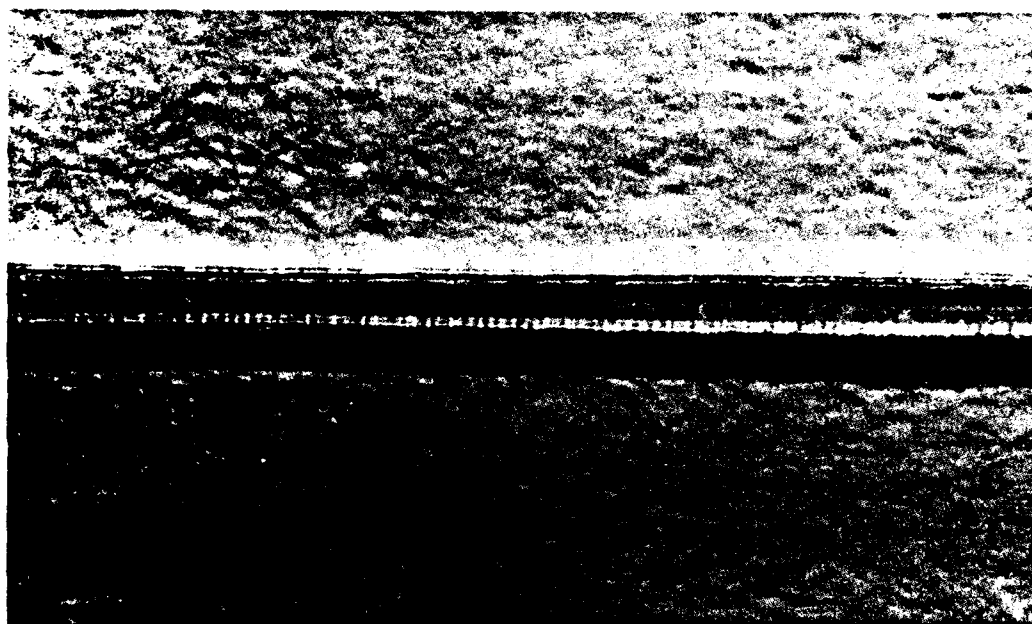


Fig. 18 Optical micrograph of a ScTaO_4 fiber, all of which have been found to be in the high temperature metastable zircon phase which has tetragonal ($4/\text{mmm}$) symmetry.

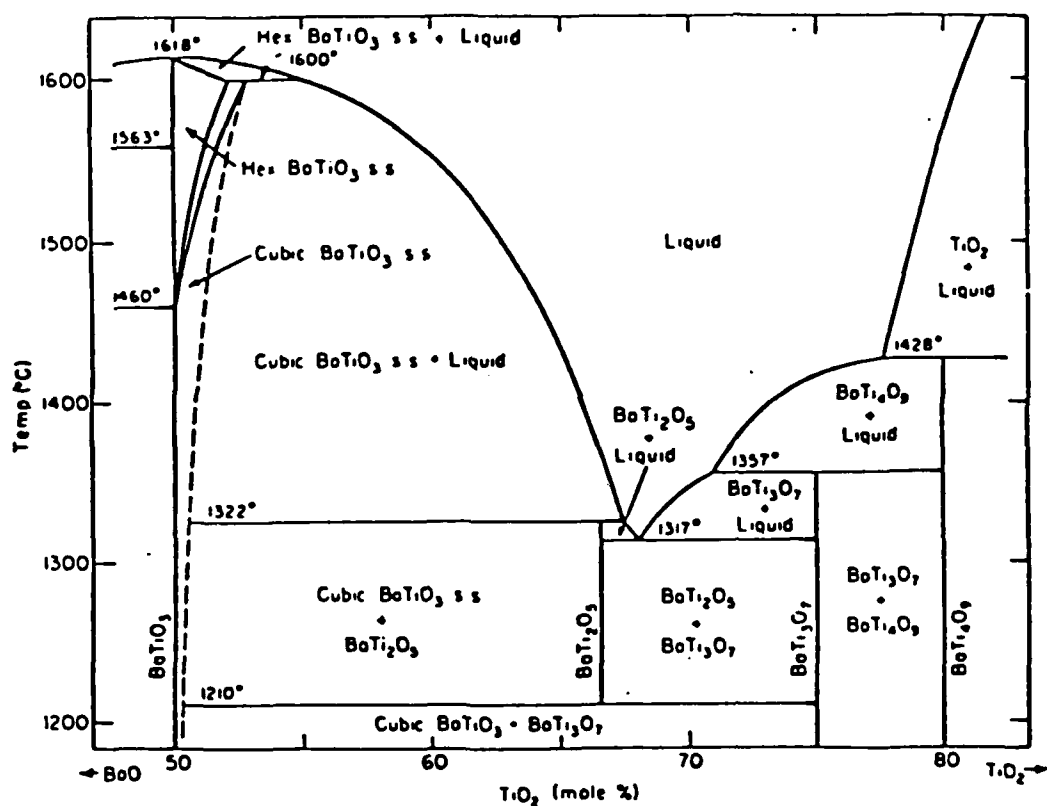


Fig. 19 Partial phase diagram of the BaO-TiO₂ system after Rase and Roy. In equilibrium, above 1460° C, BaTiO₃ is found in the hexagonal non-ferroelectric phase.

BaTiO₃

[500 μ m

Fig. 20 Optical micrograph of a metastable hexagonal BaTiO₃ single crystal fiber grown from a hot-pressed polycrystalline source rod.



Fig. 21 First LaB_6 single crystal fiber grown with the initial spherical retroreflector in place. Laser power fluctuations caused diameter variations.

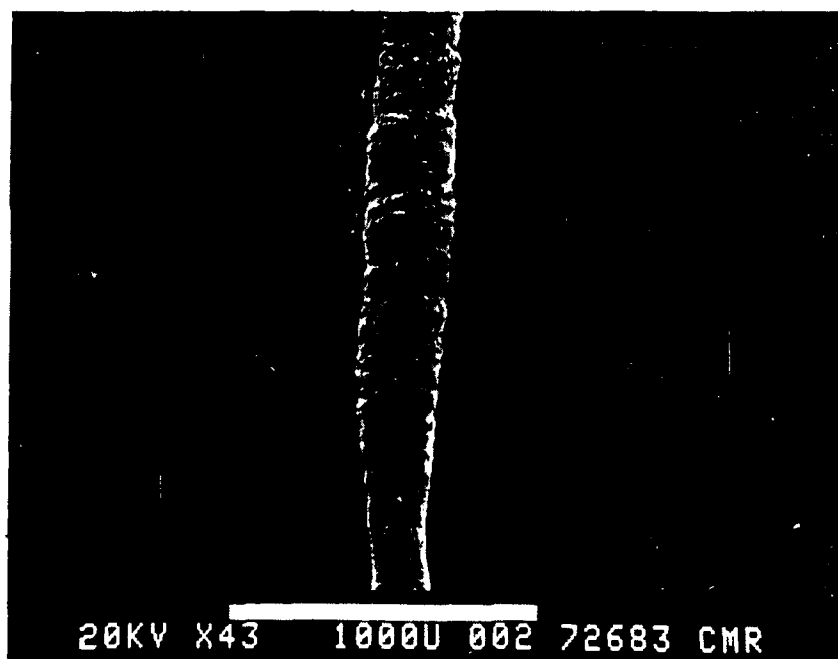


Fig. 22 Scanning electron micrograph of the first niobium metal single crystal fiber grown from a 0.030" diameter feedwire. Laser power fluctuations again caused diameter variations.

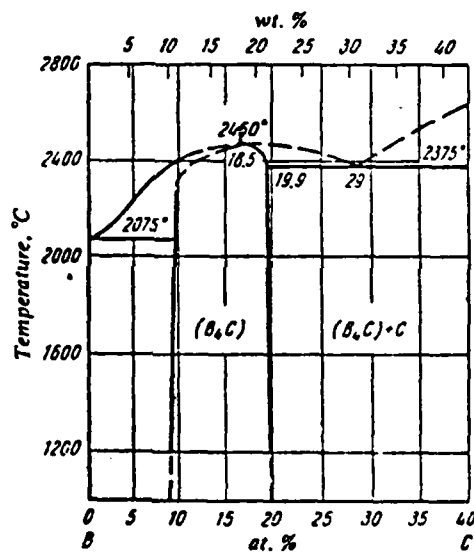


Fig. 23 Partial phase diagram of the B-C system showing the broad existence region of the rhombohedral B₄C-type phase, after G. V. Samsanov and I. M. Vinitskii, from Handbook of Refractory Materials, Plenum Press (1980), p. 525.



Fig. 24 Scanning electron micrograph composite of the first B₉C single crystal to be grown from the melt by any technique.



MISSION of Rome Air Development Center

RADC plans and executes research, development, test and selected acquisition programs in support of Command, Control, Communications and Intelligence (C³I) activities. Technical and engineering support within areas of competence is provided to ESD Program Offices (POs) and other ESD elements to perform effective acquisition of C³I systems. The areas of technical competence include communications, command and control, battle management, information processing, surveillance sensors, intelligence data collection and handling, solid state sciences, electromagnetics, and propagation, and electronic, maintainability, and compatibility.

END

FILMED

7-85

DTIC